WARMINGUP

Innovatief Duurzaam Warmtecollectief

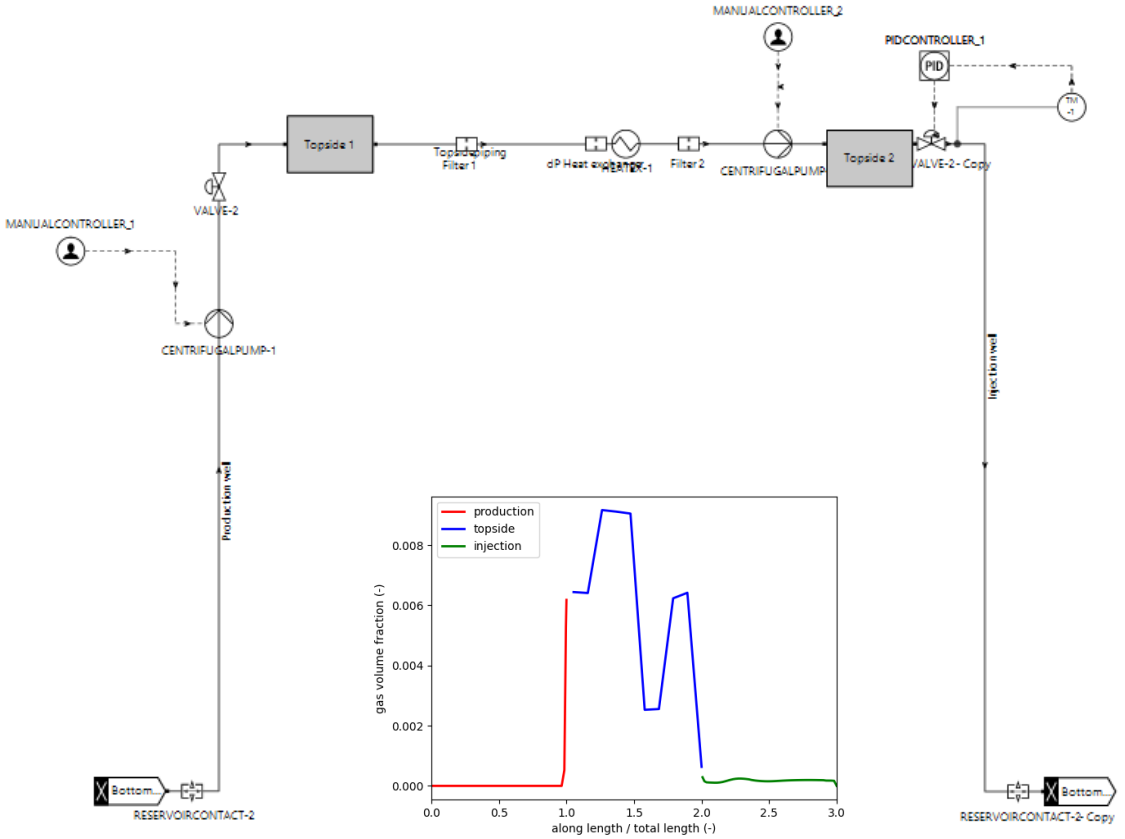

Handling greenhouse gases from geothermal wells

by

Dries van Nimwegen, Jos van ’t Westende, Pejman Shoeibi Omrani, Laura Wasch and Elisabeth Peters

24 November 2022

Including 'Addendum' by Darren Jones and Dries van Nimwegen

21 December 2023

Handling greenhouse gases from geothermal wells

Dries van Nimwegen, Jos van ’t Westende, Pejman Shoeibi Omrani, Laura Wasch and Elisabeth Peters
24 November 2022

Including 'Addendum' by Darren Jones and Dries van Nimwegen
21 December 2023

Dit project is uitgevoerd als onderdeel van het Innovatieplan WarmingUP. Dit is mede mogelijk gemaakt door subsidie van de Rijksdienst voor Ondernemend Nederland (RVO) in het kader van de subsidieregeling Meerjarige Missiegedreven Innovatie Programma’s (MMIP), bij RVO bekend onder projectnummer TEUE819001.
WarmingUP geeft invulling aan MMIP-4 – Duurzame warmte en koude in gebouwde omgeving en levert daarmee een bijdrage aan Missie B – Een CO_2-vrije gebouwde omgeving in 2050.

Projectnummer
060.43190/01.01.01

Keywords
Sand production, completions, erosion, Brussels Sand

Jaar van publicatie
2023

Meer informatie
Lies Peters
E Lies.peters@tno.nl

Table of contents

Summary

The brine produced in geothermal wells usually contains dissolved greenhouse gases (CO_2, methane and Nitrogen). Due to the changes in the system pressure and temperature, from the reservoir to the top-side, part of the dissolved gas will be exsolved. When using a topside separator, these gases can be removed from the brine. If they are subsequently discharged (either before or after burning the methane in order to generate additional heat and electricity) the greenhouse gases contribute to the overall emissions from the geothermal system. Furthermore, if the emission of these greenhouse gases is priced, this can mean a significant additional expense. Thus, mishandling of the dissolved greenhouse gasses could lead to additional cost, emissions or loss of revenues for geothermal operators.

In the current report, three strategies to handle these greenhouse gases are investigated: (1) keeping the system under pressure and never separating the greenhouse gases from the brine, (2) burning the methane (in a combined heat and power plant or in a boiler) and capturing the CO_2 and (3) separating the methane from the other gases and selling it, and reinjecting the other gases.

The result of the analysis is that option (2) is not cost effective with the current state of technology and CO_2 prices: if one or two geothermal wells are considered the relatively small scale of the carbon capture plant leads to very high cost per ton of stored CO_2. In case of a high amount of gas in the brine and a high methane fraction within the gas, selling the methane is cost effective. It still requires separating the CO_2 from the methane using carbon capture, but more value is created by selling the methane than is required for the CO_2 capture. In other cases, keeping the system under pressure is more cost-effective compared to the other evaluated options. Especially at low gas fractions the pressure required to keep the system under pressure is relatively low (below 10 bar) and, apart from changes in pump power, the operation of the well is not much affected.

The current analysis shows that the large uncertainty in the future energy prices leads to a large uncertainty in the costs of the three considered strategies. Furthermore, the current analysis can be improved by involving operators of geothermal wells and suppliers of topside equipment and ESPs to get better cost estimates and to have a more practical idea of the details of implementing each strategy.

1 Introduction

In the Climate Agreement, it has been agreed that 1.5M houses need to be heated sustainably by 2030. Heating of these houses is currently mainly done using natural gas. Part of these houses will be heated using collective heat networks with geothermal energy as one of the sources. Within the WarmingUp project Theme 4, the goal is to accelerate the development and use of geothermal sources for use in urban heat networks.

In geothermal wells, the brine includes dissolved greenhouse gases such as methane and CO_2. In the separator which is typically present in the topside facilities, the gas is removed from the brine. In most current systems, the gas is burned in a CHP (combined heat and power plant) and the resulting heat and CO_2 used in the greenhouses (Dinkelman et al., 2021). For urban heat networks, the CO_2 is likely to be vented. However, venting these gases into the atmosphere, even after combustion of the methane, will still lead to significant amounts of greenhouse gas emissions from these geothermal systems. A recent overview of these emissions for the Dutch sector is presented in Dijkstra et al. (2020) and Dinkelman et al. (2021).

To mitigate the greenhouse gas emissions, de Wildt (2020) performed a techno-economic evaluation of 10 different methods to handle these greenhouse gases. They are summarised in Figure 1. Roughly speaking, the gas can be sold (1), can be used in a boiler or combined heat and power plant (CHP) in combination with carbon capture, or can be kept in solution. The CO_2 can be co-injected into the injector well or transported elsewhere for utilization. From the work of de Wildt three options seemed most promising:

- Keeping the entire system under pressure, such that the greenhouse gases never come out of solution.
- Using a CHP in combination with carbon capture and injection of the carbon dioxide into the injection well.
- Separating the greenhouse gases, and selling the methane. The CO_2 can be sold or re-injected.

In this work, these three options are worked out further. A separate chapter will be devoted to each of the three options.

In the case of keeping the system under pressure, simulations are performed in pipeline flow simulator OLGA[(2)] to better understand the impact of different operational conditions on the system. The effects of the gas to liquid ratio (GLR) and the brine composition are determined. Furthermore, the effects of the reservoir pressure and the gas composition are studied.

In the case of the CHP in combination with the carbon capture, the goal of the work is to determine whether the carbon capture is feasible, from a techo-economic perspective, when the CO_2 from two wells with a large GLR is captured. This required an investigation of the scaling of the cost with the amount of CO_2 that is captured. Furthermore, it was determined whether adding the CO_2 coming from the 'bijstook' (3) to the injection can make it a financially and technically viable option.

[1] Strictly speaking the sales of methane does not reduce the global GHG emissions if there is no means of CCS at the location where it is used, but it avoids using alternative fossil natural gas, thus being an indirect reduction.
[2] OLGA is a commercial 1D simulator for gas/liquid flows in pipeline systems.
[3] 'Bijstook' is the burning of gas for providing additional heat during the cold season when the heat from the geothermal system is insufficient (i.e. to serve the peak demand). This is done in other installations (i.e. not at the geothermal location).

In the third chapter, the greenhouse gasses are separated from the brine and then further split into CO_2, CH_4 and other components. The CH_4 is then sold to the market. It is determined whether this could be profitable. Note that the sale of the CO_2 is not considered and the emission of the party buying the methane is considered out of scope of the current analysis.

Since the assessment of the various options differs, they cannot be compared directly. Instead an attempt is made to assess the impact of a certain option with respect to a relevant base case, which can differ per option.

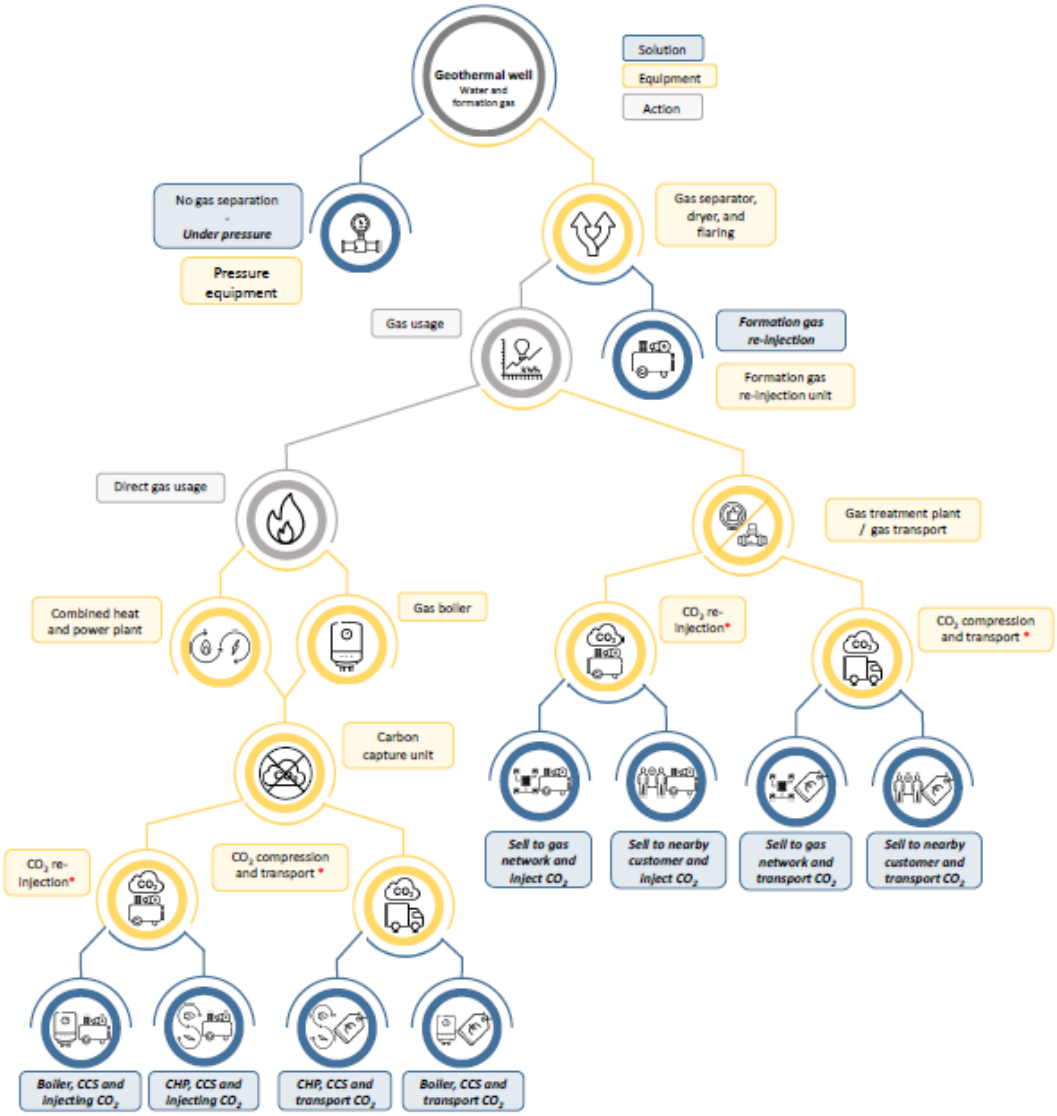

Figure 1: Overview of options presented by de Wildt (2020) to handle greenhouse gases.

2 Under pressure

An option for handling the greenhouse gases in geothermal wells is to keep the system under pressure such that the gasses never come out of the solution. This requires that all topside facilities are able to withstand the higher pressure, which increases the CAPEX. Furthermore, the ESP needs to increase the pressure in the production well further, leading to a higher OPEX and possibly CAPEX costs for this pump. Finally, the injection pump no longer requires the pressure to be increased as much since the pressure at the topside is already much higher and this can lead to a decrease in OPEX or even CAPEX (if the injection pump can be removed).

2.1 Determining the gas fraction

The pressure that is required to keep all greenhouse gases in solution depends on both the amount of gas present in the brine, but also on the brine and gas composition. An equation of state is required in order to predict the vapour-liquid equilibrium (VLE) [4]. In this work, two software programs are used in order to obtain the properties of the brines: PVT Sim and PHREEQC (Parkhurst & Appelo, 2013). PVT Sim was created for the oil-and-gas industry and allows the calculation of the fluid properties of many hydrocarbons. However, relatively few salt components are present to simulate the brine properties. PHREEQC is a program specifically designed for the simulation of aqueous geochemical solutions and therefore has many options for the simulation of chemically complex brines.

To show which program is most suitable to calculate the gas fraction and the bubble point pressure, a comparison was made with literature data for the bubble point obtained from Lucile et al. (2012) for CO_2 in water, from Culberson & McKetta (1951) for methane in water and from Duan et al. (1992) for methane in brine. This comparison is made in Figure 2, Figure 3, and Figure 4, respectively.

For the PVT Sim calculations the SRK Peneloux (T) equation of state was used, in combination with a Huron-Vidal mixing rule for the polar components. The PHREEQC results were obtained with the default PHREEQC database.

For pure water, PVT Sim is very good at calculating the bubble point pressure for both methane and CO_2. It is only at the higher brine concentrations that PVT sim fails to accurately predict the bubble point pressure (see Figure 4). As shown in Figure 5, the salinity in most Dutch gas wells is too high for PVT Sim to be able to accurately predict the gas solubility with typical salinities of 100-300 g/l.

Furthermore, in PVT Sim only a few different salts are available to make up the brine. In PHREEQC there are many more possibilities. In PHREEQC it is also possible to calibrate the gas fraction based on a sample taken from a geothermal well, leading to better results of the actual calculation of the gas fraction.

[4] The vaporous phase includes both the dissolved gases that have come out of solution as water vapour.

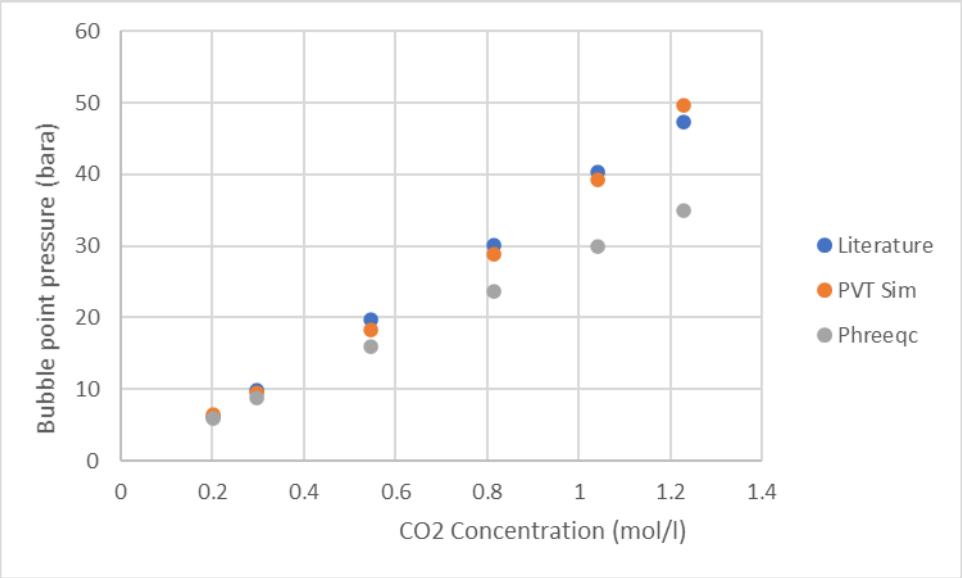

Figure 2: Bubble point pressure as a function of the CO_2 concentration in pure water at a temperature of 25°C.

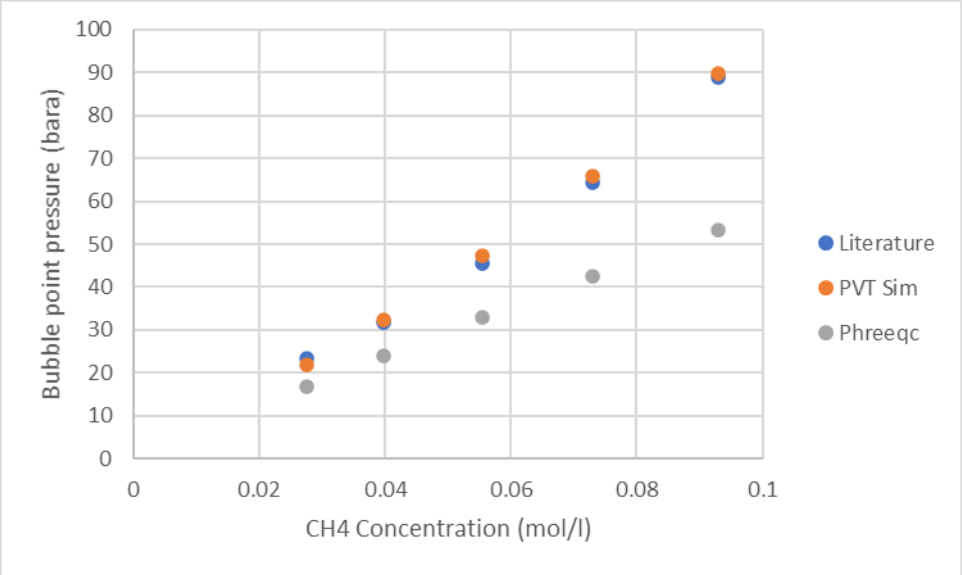

Figure 3: Bubble point pressure as a function of the CH_4 concentration in pure water at a temperature of 25°C.

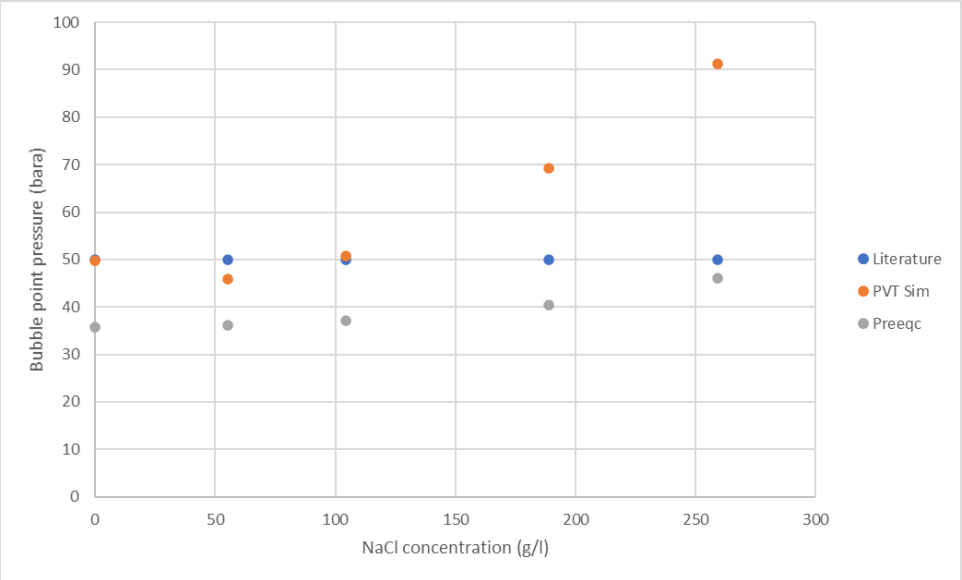

Figure 4: Comparison of the bubble point pressure for CH4 in sodium chloride solutions.

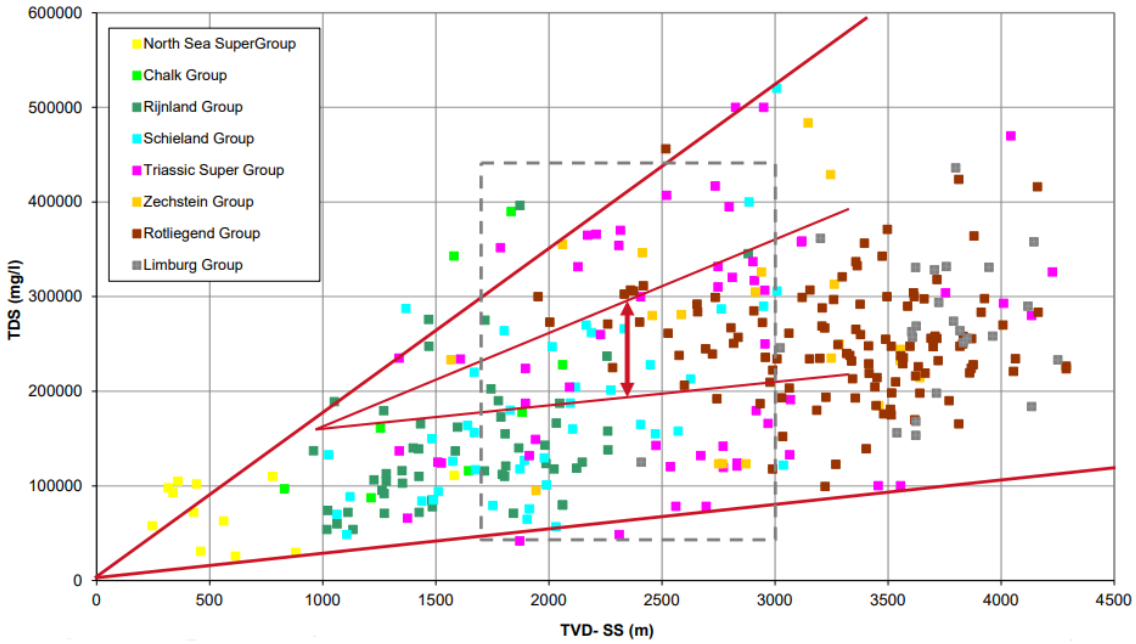

Figure 5: Salinity of gas wells in the Netherlands, data taken from www.nlog.nl (Veldkamp et al., 2015).

In the current work, flow simulations will be performed with fluid property data based on field brines. These simulations are performed in OLGA, a commercial software package used in the oil and gas industry that contains a 1D multiphase flow solver. A method to include the PHREEQC calculations in the OLGA simulations was developed. In the calculations for the reservoir brines, the Pitzer database in PHREEQC is used, which is well suited for simulating gas solubilities at high salinity. This method is presented in Appendix A. The used fluid and gas composition and the PHREEQC model setup can be found in Appendix B.

2.2 Calculated gas fractions and densities

For the flow simulations two brine compositions and three gas-to-liquid ratios are considered. The brine compositions are taken from fluid compositions determined from well samples that are available for download from nlog.nl. The first water sample is from the Middenmeer geothermal doublet, and the second sample is from the Heemskerk geothermal doublet. In the PHREEQC calculations three different gas fractions are considered for these brines. Based on the data on geothermal wells in the Netherlands presented in Figure 6 gas-to-liquid ratios (GLR) of 0.33 Nm^3/m^3 and 1 Nm^3/m^3 are selected. To show the extreme of what is possible in a well, additionally a GLR of 1.5 Nm^3/m^3 is considered. Both the Heemskerk site and Middenmeer site represent GLR of around 0.33 Nm^3/m^3, as the plants produce from the Permian-age Slochteren-sandstone. Hence the extrapolation to higher gas-to-liquid ratios is hypothetical, as a resulting change in initial water pH and accompanying different water composition is not taken into account.

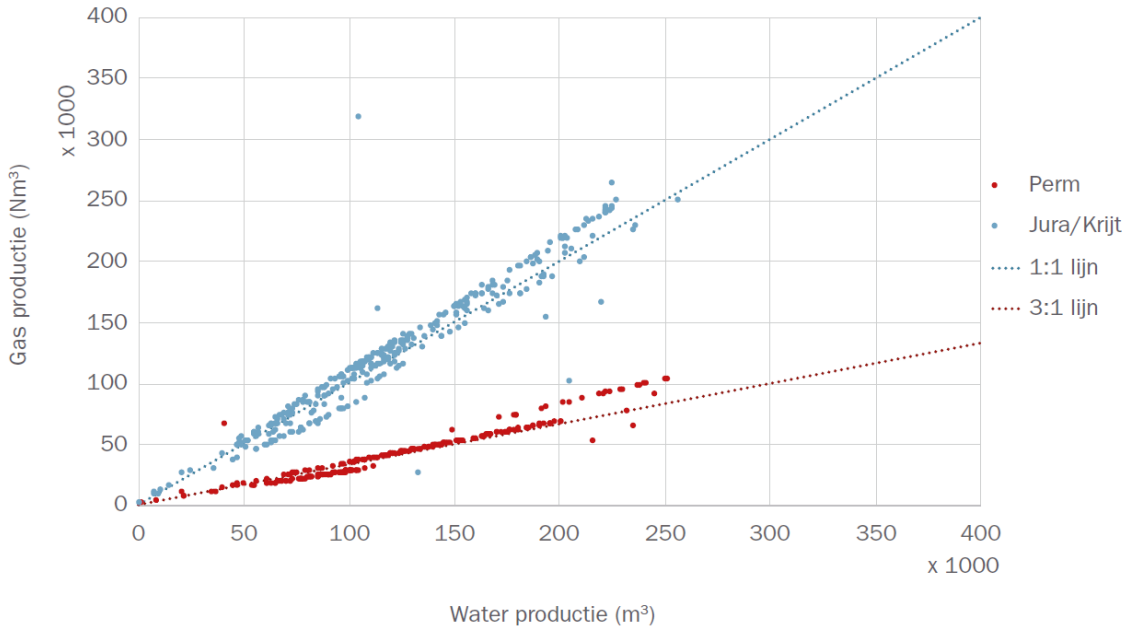

Figure 6: Gas-to-liquid ratios for geothermal wells in the Netherlands (Dijkstra et al., 2020).

The results for the calculated density of the two brines is presented in Figure 7. For both brines the density decreases with temperature and increases with pressure, as is expected. However, the brine in Heemskerk weighs about 100 kg more per cubic meter. This significantly changes the hydrostatic pressure gradient, which can have a large effect on the required pumping power in the ESP. In Figure 8 the gas fraction is presented as a function of pressure and temperature for a GLR of 0.33 Nm^3/m^3. The results show that the gas volume fraction [5] quickly drops at low pressures, to only 5% or less at a pressure of 5 bar. However, at a temperature of 90 °C (close to the temperature at which the brine is often produced) a pressure of about 10 bar is required in order to limit the gas volume fraction to 1%, while a pressure of over 15 bar is required to dissolve all gas. There is quite a long tail of pressures for which a little bit of gas remains as free gas.

[5] When a fluid consists of both liquid and free gas, a liquid and gas volume fraction can be defined. Each of the volume fractions has a value between 0 and 1, and the sum of the volume fractions is always equal to 1.

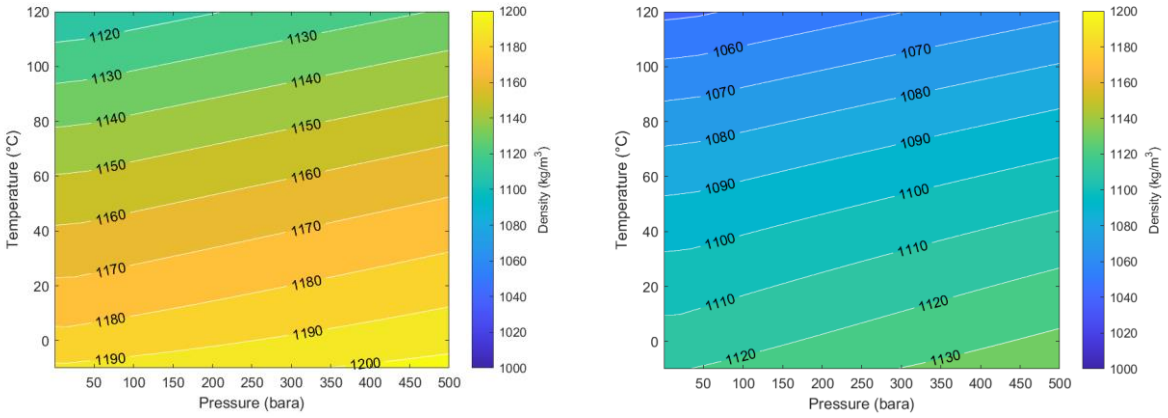

Figure 7: Density as a function of pressure and temperature for the Heemskerk brine (left) and for the Middenmeer brine (right).

In Figure 9 the gas fraction is presented only as a function of pressure for the three GLR values and for both brines (Middenmeer and Heemskerk) at temperatures of 25 °C and 90 °C. It shows that the GLR has a large effect on the pressure required for all gas to be in solution, which is consistent with the data presented in Figure 4. Furthermore, the temperature has a significant effect: at a GLR of 1 Nm^3/m^3 and a temperature of 25°C the gas is fully dissolved at 30 bar, while at 90 °C more than 40 bar is required. This indicates that the largest problems with keeping the gas in solution will occur just upstream of the heat exchanger.

The pH of a brine is controlled by the water composition, CO_2 concentration, temperature and mineral reactions. Note that the reactions are not taken into account in the current study, but that calcite precipitation is of concern in case of significant outgassing. Since the gas contains a significant fraction of CO_2 (about 10 mole % for Middenmeer brine and 25 mole % for the Heemskerk brine), the gas fraction is the dominant control on the pH of the solution. Results for the pH are presented in Figure 10. Clearly the Heemskerk brine is more acidic due to the larger CO_2 fraction. For all solutions, the acidity decreases at low pressure as the gas comes out of solution. In Figure 11 the pH is shown for only lower pressure, to better show the comparison of pH with the free gas fraction in Figure 8.

Overall, this section shows that using PHREEQC and based on the brine analysis and the gas fraction, the liquid density and the pH of a brine can be determined as a function of pressure and temperature. These results show that the brine composition has a significant effect on the liquid density, while the GLR affects both the gas fraction and the pH. In the next section, OLGA simulations will be run with these brines to show the effect of the properties calculated in PHREEQC on the flow in a geothermal doublet.

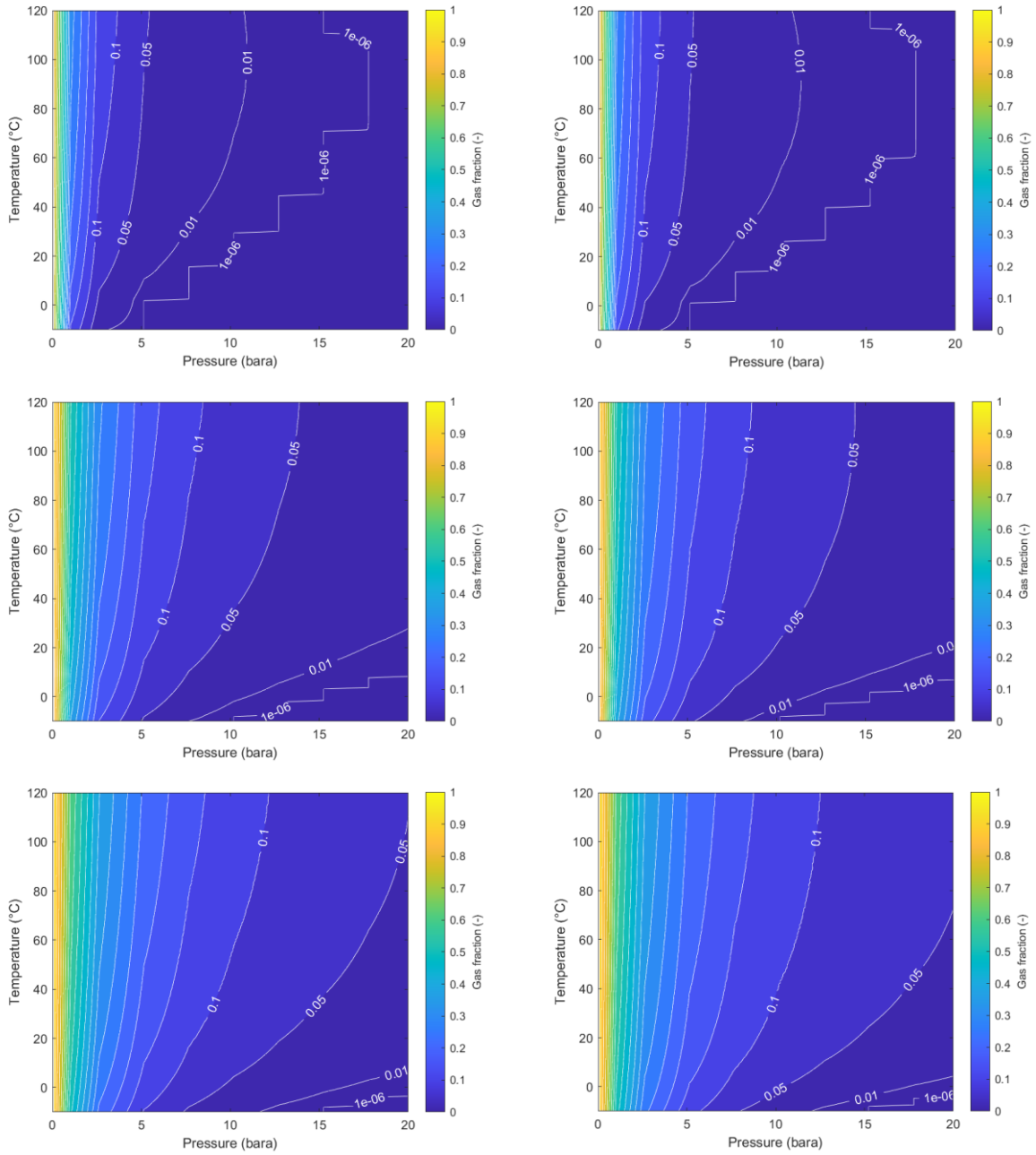

Figure 8: Gas fraction present as free gas as a function of temperature and pressure for the Heemskerk (left) and Middenmeer (right) wells. The top two figures show the results for an GLR of 0.33 Nm3/m3. In these figures the two rightmost white lines indicate when the gas fraction is reduced to 1% and to 0%. The second and third row of figures show results at gas fractions of 1 Nm3/m3 and 1.5 Nm3/m3, respectively.

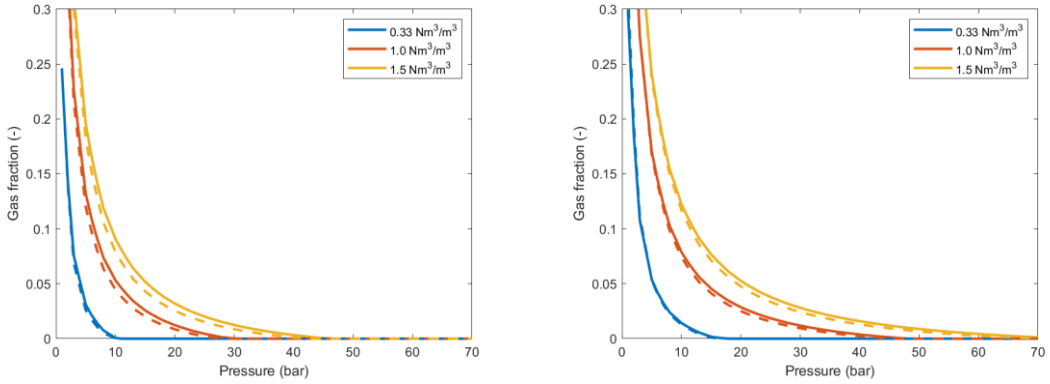

Figure 9: Gas fraction as a function of the temperature for the three gas-to-liquid ratios considered for a temperature of 25°C (left graph) and a temperature of 90°C (right graph). The solid lines indicate the results for Middenmeer, the dashed lines indicate the results for Heemskerk.

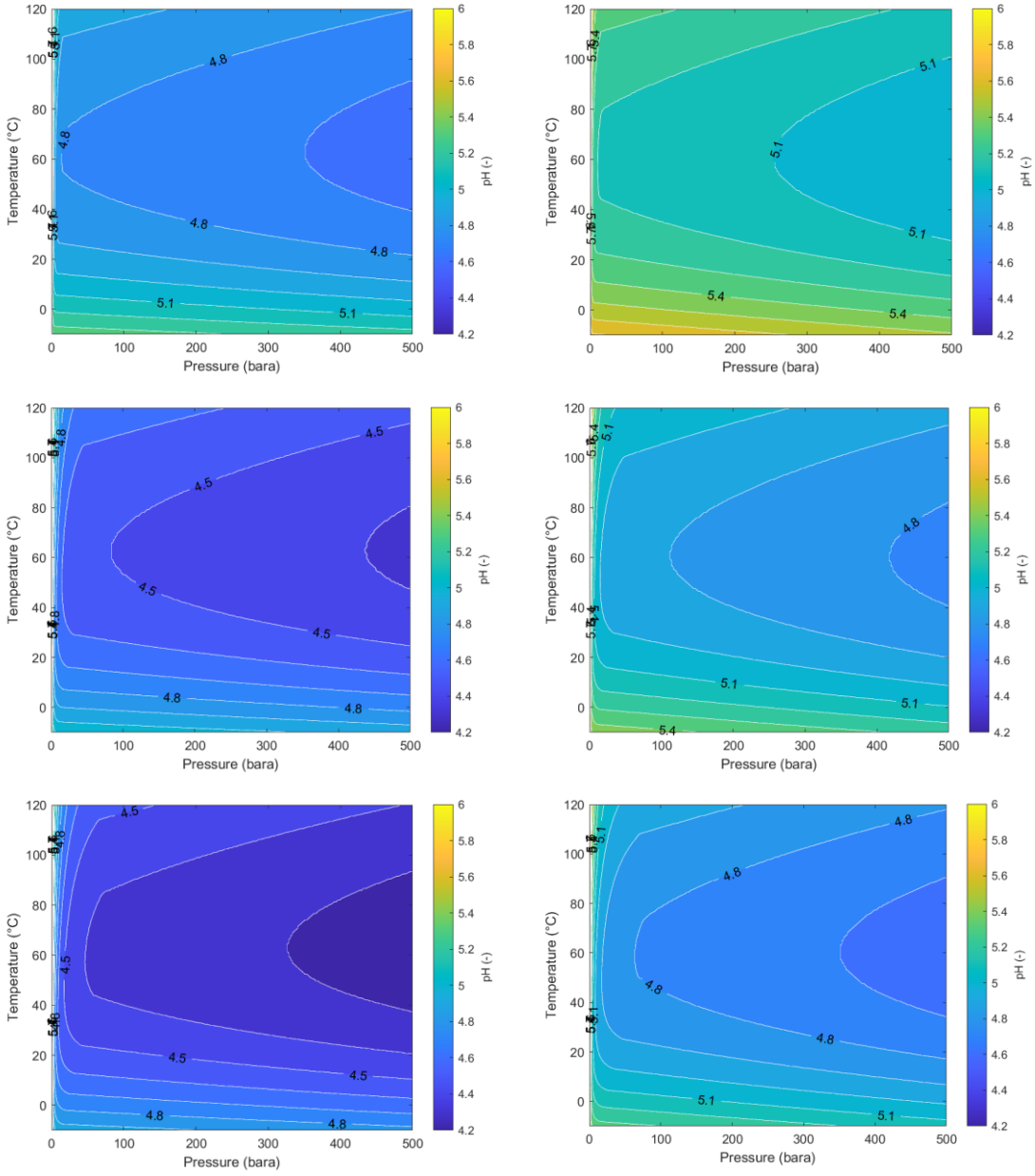

Figure 10:The pH as a function of pressure and temperature for the Heemskerk brine (left column) and the Middenmeer brine (right column). Each for three values of the gas-liquid ratio (from top to bottom): 0.33 Nm3/m3, 1.0 Nm^3/m^3 and 1.5 Nm^3/m^3.

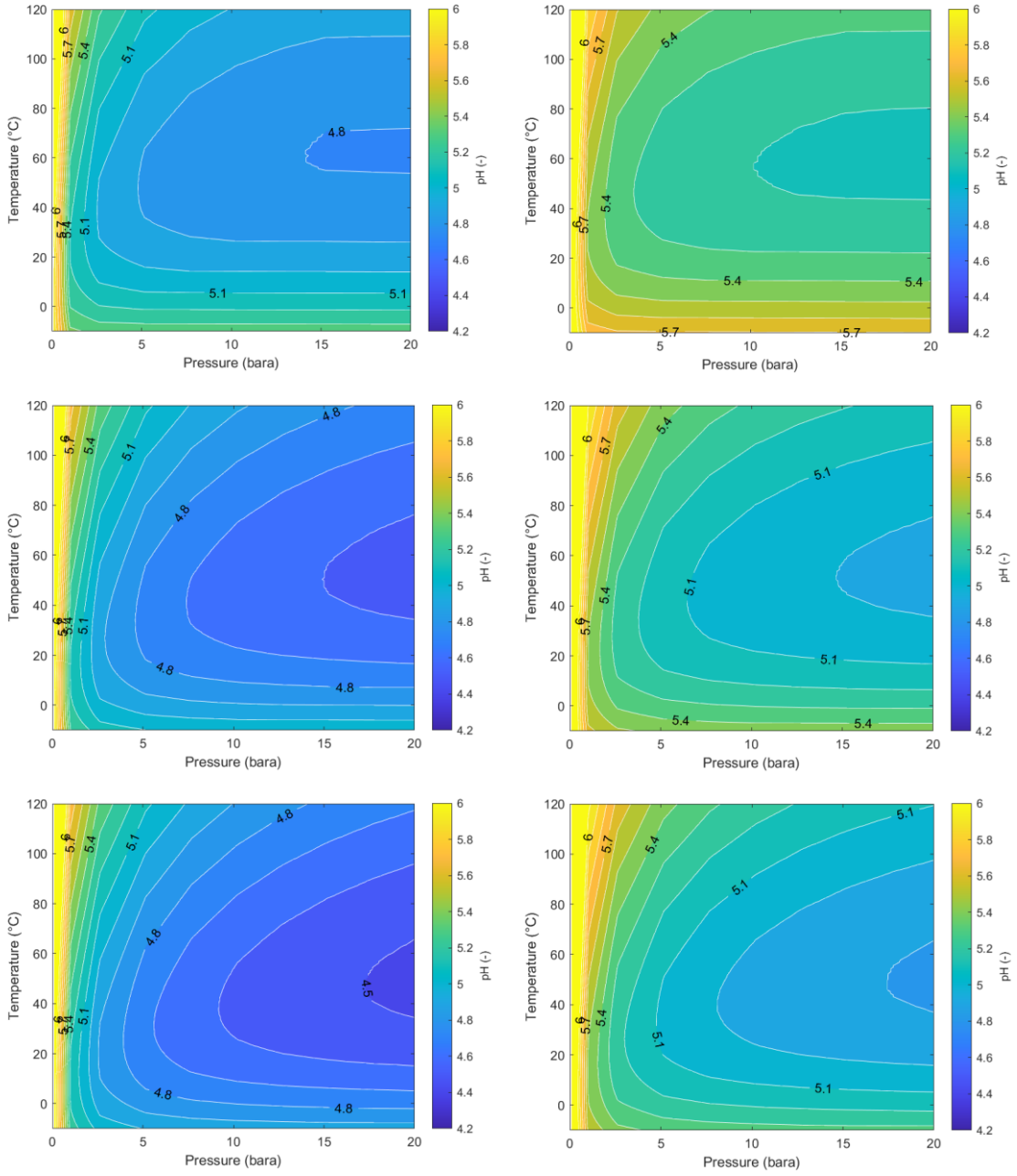

Figure 11: The pH as a function of pressure and temperature for the Heemskerk brine (left column) and the Middenmeer brine (right column). Each for three values of the gas-liquid ratio (from top to bottom): 0.33 Nm3/m3, 1.0 Nm^3/m^3 and 1.5 Nm^3/m^3. This figure shows results at low pressures for comparison with Figure 8.

2.3 OLGA Simulations

For the simulations a geothermal doublet is modelled as shown in Figure 12. This model is used to simulate the flow in the geothermal well in order to determine the gas fraction occurring in the topside under various conditions. The design is simplified and only shows the key components of the system. The wells are both vertical, and contain a production zone of 200 meters, with a reservoir

contact in the middle. At the top of the production well, a tubing with a length of 800 m is placed that has an ESP installed at the bottom. The ESP is modelled as a centrifugal pump using data from an actual ESP as shown in Figure 13. For the ESP the head is multiplied with a factor of 1.5 with respect to the values in Figure 13, in order to obtain sufficiently high pressures in the topside to keep the gas in solution in the coming calculations. The topside valve in the injection well is used to control the flow rate (when required). The internal diameters of the system components can be found in Table 1.

Table 1: Internal diameter of the components in the system.

Component	Internal diameter (m)
Bottomhole	0.15
Liner	0.22
Tubing	0.14
Topside piping	0.20

At the topside four components are placed: two filters and a heat exchanger. For the heat exchanger the output temperature is fixed at 30°C. Each of the components (filters 1 and 2 and the heat exchanger) have a pressure drop included. The pressure drop, ΔP, is modelled using a coefficient, ζ, which can be found in Table 2:

$$\Delta P = \zeta \ \tfrac{1}{2} \rho U^2$$

Where ρ is the density of the brine, and U is the flow velocity of the brine based on an inner diameter of 0.2 m.

Table 2: Pressure loss coefficients of the topside facilities.

Component	Coefficient (ζ)	Pressure drop at 250 m3/h (bar)
Filter 1	42	1.1
Heat Exchanger	56	1.5
Filter 2	42	1.1

In the example case in the simulations the data in Table 3 will be used. The reservoir pressure in this example case, based on the Heemskerk well, is relatively low. The hydrostatic pressure gradient of the liquid in the well alone is already larger than the reservoir pressure. This is the reason for placing the ESP 800 meters below the ground: for an ESP at 500 meters depth there would be gas at the ESP inlet.

Table 3: Data obtained from nlog.nl for the Heemskerk doublet, which will be used in the base case simulations.

Quantity	Value
Well depth (TVD)	2500 m
Reservoir pressure	250 bar (@2400 m depth)
PI	2.71×10^{-5} kg/s Pa

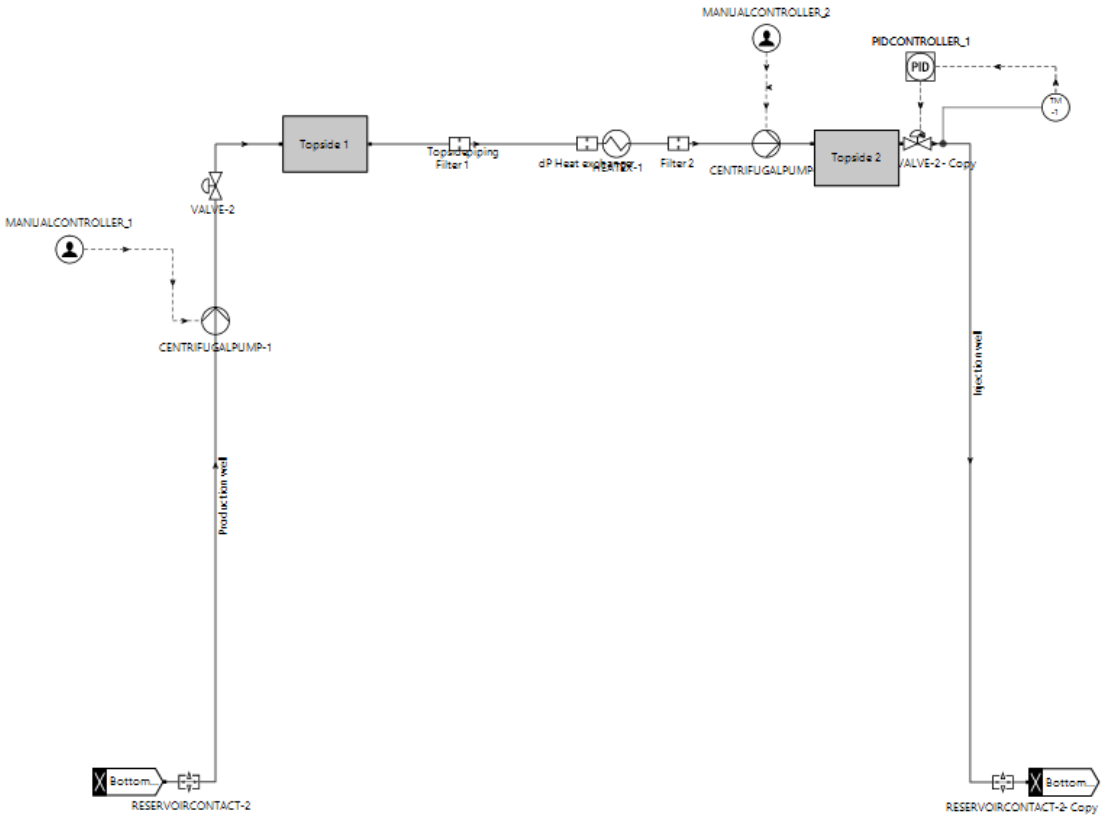

Figure 12: Geothermal doublet as modelled in OLGA.

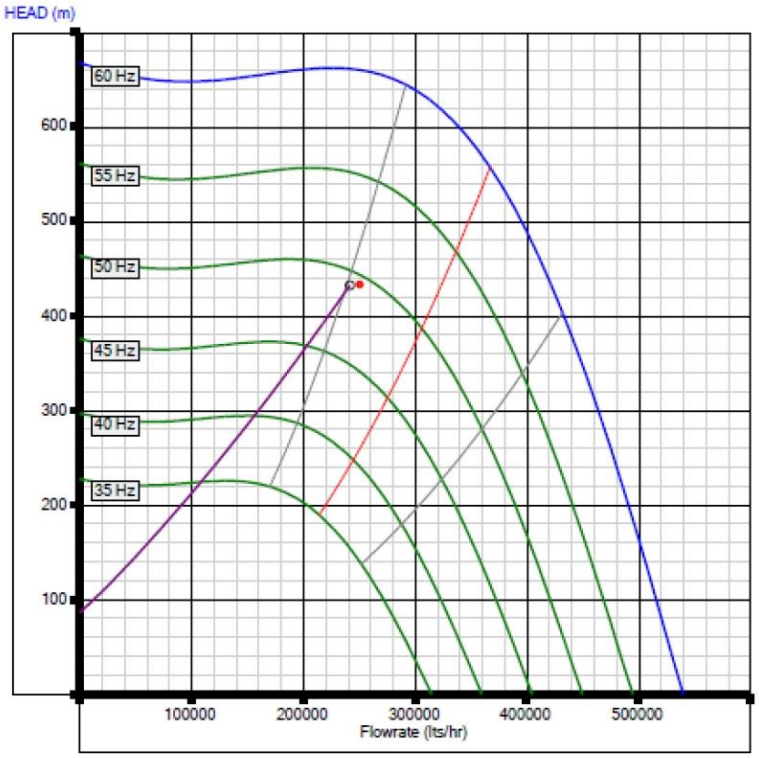

Figure 13: Pump curve for the ESP used in the current model. The head values are multiplied by 1.5 for the simulations in this chapter.

In this section the required pressure in the topside facilities is determined. A higher pressure at the topside would lead to higher cost in constructing the topside facilities. Furthermore, it requires more power from the ESP leading to a more costly ESP. An ESP is also less energy efficient than a topside injection pump. However, a too low pressure at the topside leads to a larger gas fraction, which can cause problems in the filters, heat exchangers and the pump. Especially pumps are very sensitive to larger gas fractions. At very low gas fractions the small bubbles move along with the liquid in the pump and there are no major problems. However, as the gas fraction increases the bubbles agglomerate and will move slower than the liquid. Due to this phase slip the liquid flow rate through the pump decreases. Above a critical gas fraction the pump becomes gas locked. At this point the gas fraction locally in certain parts of the pump, specifically in the impellor passage, reach 100% and the impellor tries to displace air (Jiang et al., 2019). The critical gas fraction depends on the pump design and occurs at gas fractions of 4-30% (see the examples from Figure 14).

In Figure 14 the decrease in relative pump performance is shown as a function of the gas volume fraction at the inlet. All results show a rapid decrease of the pump performance at low volume fractions. In this work, it is assumed that for a gas volume fraction of at most 1%, the pump performance is hardly affected by the gas. Therefore, in this report the gas fraction at the inlet of the injection pump is never allowed to be larger than 1%. Note that this is a conservative estimate and depending on the pump type a larger inlet gas fraction may be possible.

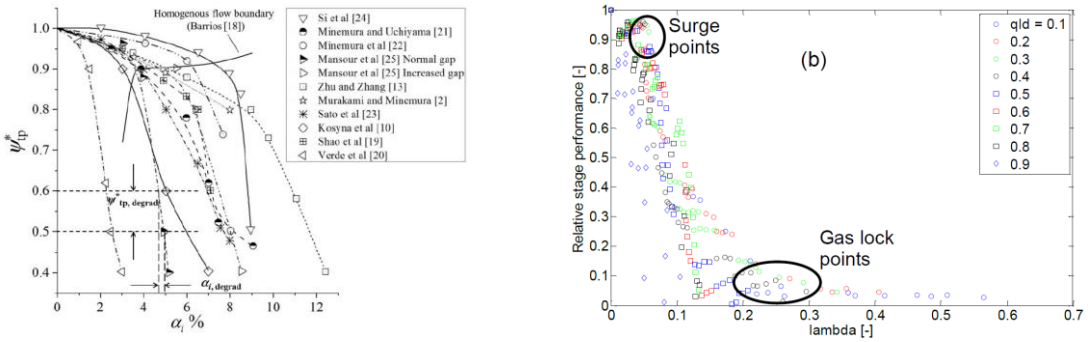

Figure 14: Examples of the relative pump performance as a function of the gas volume fraction, α_i, for centrifugal pumps (left, Jiang et al., 2019) and for ESPs (right, this graph was created using data from Gamboa & Prado (2012)). At a no-slip gas volume fraction (lambda) of 0.25 and higher the stages are experiencing gas-lock.

Besides the pump, the topside also contains heat exchangers and filters. The exact effect of the gas volume fraction on these components depends on their design. For vertically oriented plate heat exchangers it has been observed that the presence of bubbles can actually increase the heat transfer as the bubbles increase the mixing of the warm fluid in the center with the colder fluid at the wall (Dabiri & Tryggvason, 2015). For low gas fractions, typically the slip between the phases is limited and a gas volume fraction of less than 1% should not have a big impact on the performance of the filters and the heat exchanger.

In Figure 15 the simulated gas volume fraction and pressure in the entire system is shown. The three colours indicate the three pipe sections (production well, topside and injection well). Note that each of the lengths of the pipe sections has been normalized to 1, hence the picture is not to scale. The settings of the ESP and the injection pump are tuned in such a way that the gas fraction at the topside is never larger than 1% for a liquid flow rate of 245 m^3/h.

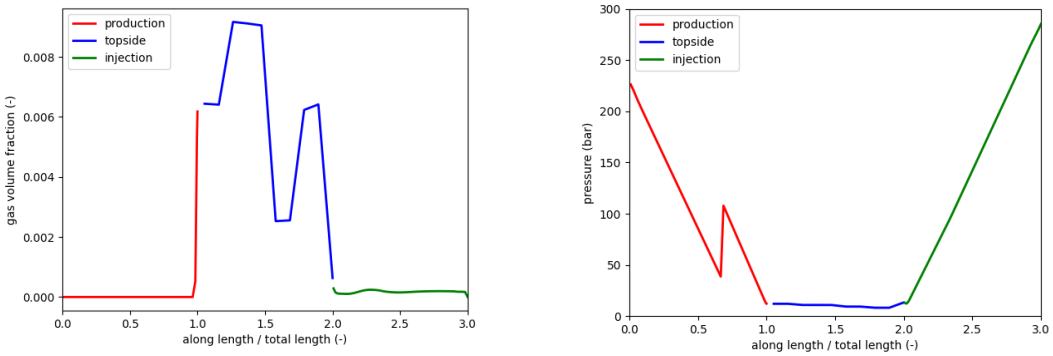

Figure 15: Gas volume fraction and pressure in the system for the base case based on Heemskerk with a GLR of 0.33 Nm^3/m^3 and an ESP speed of 50 Hz and an injection pump speed of 30 Hz.

From the OLGA simulations, the power usage of the two pumps can be calculated, assuming a certain pump efficiency. In line with results from Van 't Spijker & Ungemach (2016) an efficiency of 55% is selected for the ESP, while an efficiency of 70% is assumed for the injection pump, in line with the work of Wildt (2020). For this example, this leads to a power usage of 923 kW for the ESP and 56 kW for the injection pump. It is the relatively low reservoir pressure that causes the big difference in pump power: there is almost no pressure required to drive the liquid into the reservoir. The pressure just upstream of the injection pump is 8.2 bar in this example, which can easily be managed in a pipeline system. The bubble point pressure in this system is 10.2 bar at a temperature of 30°C and 17.8 bar at a temperature of 90°C, so operation occurs at a pressure of only half the bubble-point pressure at 90°C.

Note that in the OLGA simulation presented in Figure 15 there is still a very small gas fraction left in the injection well. This is not what will happen in practice, but is something that likely occurs due to way the gas fraction is calculated in OLGA. In OLGA, developed by Schlumberger, a tab file is used to specify the fluid properties. Round-off errors in gas fraction changes from the tab file can cause gas to remain at pressures above the bubble point pressure. It was indicated by Schlumberger customer support that this could be solved by using the compositional tracking module. However, compositional tracking does not allow the changes to the tab file using PHREEQC. Therefore, it was decided to accept these small gas fractions in this project to allow the use of PHREEQC to modify the fluid property tab-files.

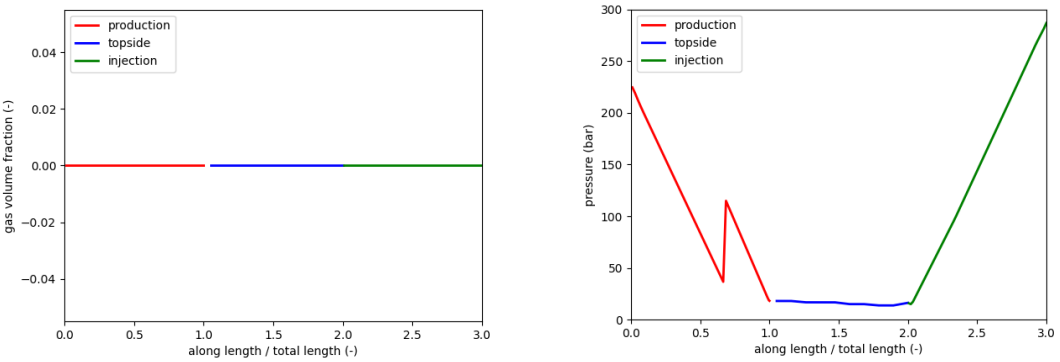

Figure 16: Holdup and pressure for the base case based on Heemskerk with a GLR of 0.33 Nm^3/m^3 and an ESP speed of 53 Hz and an injection pump speed of 30 Hz.

In Figure 16 the pump power of the ESP was increased such that the gas volume fraction is equal to zero everywhere in the system. This required a pressure just upstream of the injection pump of 13.0 bar. The power of the ESP is then 1.10 MW and the power of the injection pump is 30 kW. The flow rate in the system is 262 m^3/h, this his higher than in Figure 15 since the ESP has to pump significantly more, while the injection pump cannot be turned down any further. This example shows that allowing a gas fraction of 1% can reduce the required pressure at the topside facilities with 4.8 bar, while the power requirements van be decreased by about 0.15 MW.

2.3.1 Selecting pump speeds and calculating the required power

In the previous example, only the speed to the ESP was varied, while in general the speed of both the ESP and the injection pump can be controlled, and this determines the pressure at the topside, the liquid flow rate and the gas fraction at the topside. Contour plots can be made of these quantities as a function of the power of the two pumps, as is done in Figure 17.

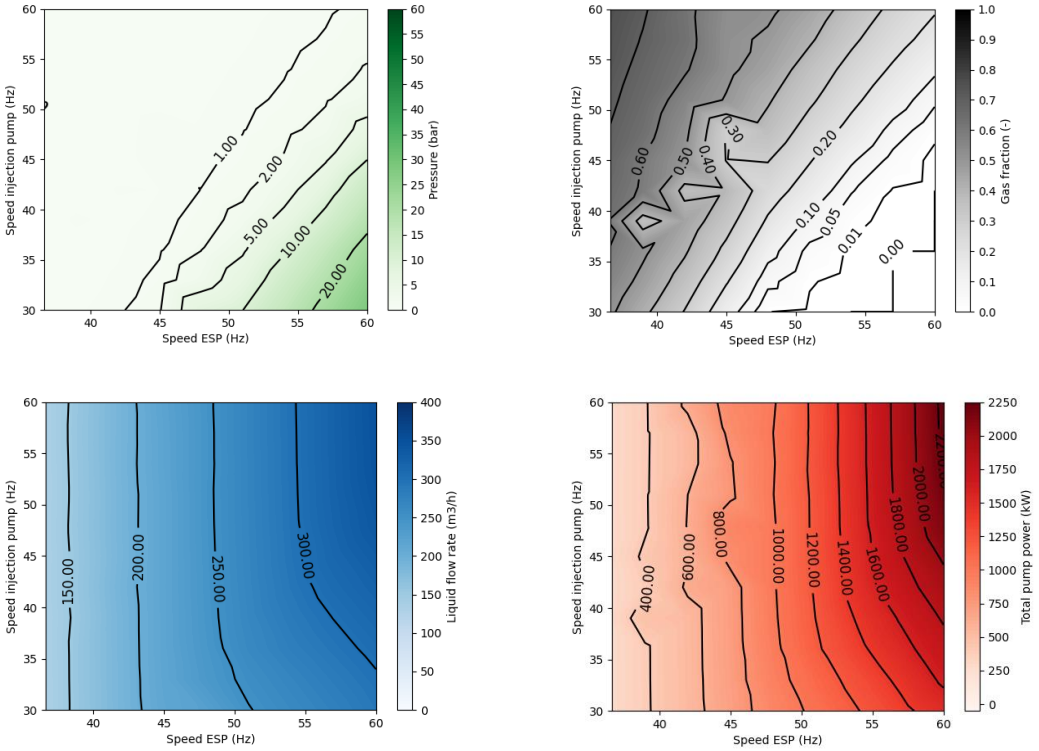

Figure 17: Contour plots of the pressure upstream of the injection pump (top-left), the maximum gas fraction at the topside facilities (top-right), the liquid flow rate (bottom-left) and the total pump power (bottom-right) for the base case.

Figure 17 shows that the gas fraction is only 0.01 or lower when the ESP power is relatively high and the injection pump power is relatively low. At high injection pump power the high flow rate leads to large pressure losses between the ESP and the injection pump, leading to a lower pressure at the inlet of the injection pump. Note that the largest pressure gradient in the system occurs in the tubing between the ESP and the topside, where the lowest pipe diameter occurs. Along the line of a gas fraction of 0.01, the system can be operated at the minimum injection pump speed for a relatively low flow rate, as was the case in the example in Figure 15. Alternately, the system can be operated at higher flow rates for which the ESP is run at full power and the injection pump is run at about 45 Hz. Note that OLGA does not decrease the flow rate through the pump as a function of the gas

fraction as much as would be expected from Figure 14. Therefore, the flow rate obtained by OLGA for the larger gas fractions is probably not reliable.

To investigate the effect of the reservoir pressure on the system, the same contour plots were also created for a reservoir pressure of 270 bar, leaving everything else in the system the same. The results are presented in Figure 18. That the pressure in the system is now 20 bar higher at the same pump power allows much more flexibility in operating the system. The contour at a gas fraction of 0.01 now lies diagonally across the plot, so the injection pump rate can be varied along its entire range. In this way a large variation of liquid flow rates can be obtained. Due to the higher flow rates, the total pump power is increased at the same pump speeds with respect to Figure 17.

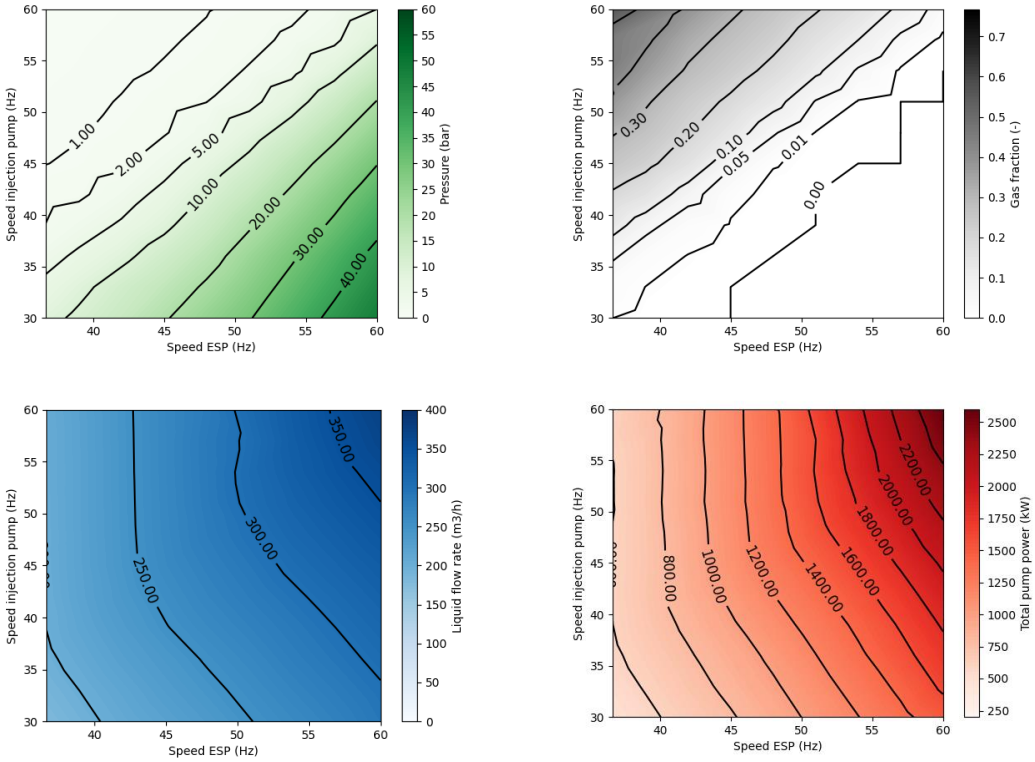

Figure 18: Contour plots of the pressure upstream of the injection pump (top-left), the maximum gas fraction at the topside facilities (top-right), the liquid flow rate (bottom-left) and the total pump power (bottom-right) for an increased reservoir pressure of 270 bar.

The simulations from the previous figures were all run for the lowest GLR or 0.33 Nm^3/m^3. To show the effect of the GLR, in Figure 19 the same contours are presented for the base case with a GLR or 1.0 Nm^3/m^3. Due to the additional gas, a lot more pressure is required to limit the gas fraction to only 0.01. For the current pumps there is only one possible mode of operation: the ESP should be at its highest setting and the injection pump should be at its lowest setting. Off course, a larger ESP could be installed in an actual well in order to have more flexibility in operation. Flow rates below 280 m3/h can only be reached in this system by choking the flow downstream of the injection pump. For these lower flow rates the injection pump would then not be required, and could be bypassed.
To investigate the effect of the brine composition, in Figure 20 contours are presented for the Middenmeer brine. Since this brine has a significantly lower density, the pressure at the same ESP speed is higher. This is equivalent to a higher reservoir pressure inside the system.

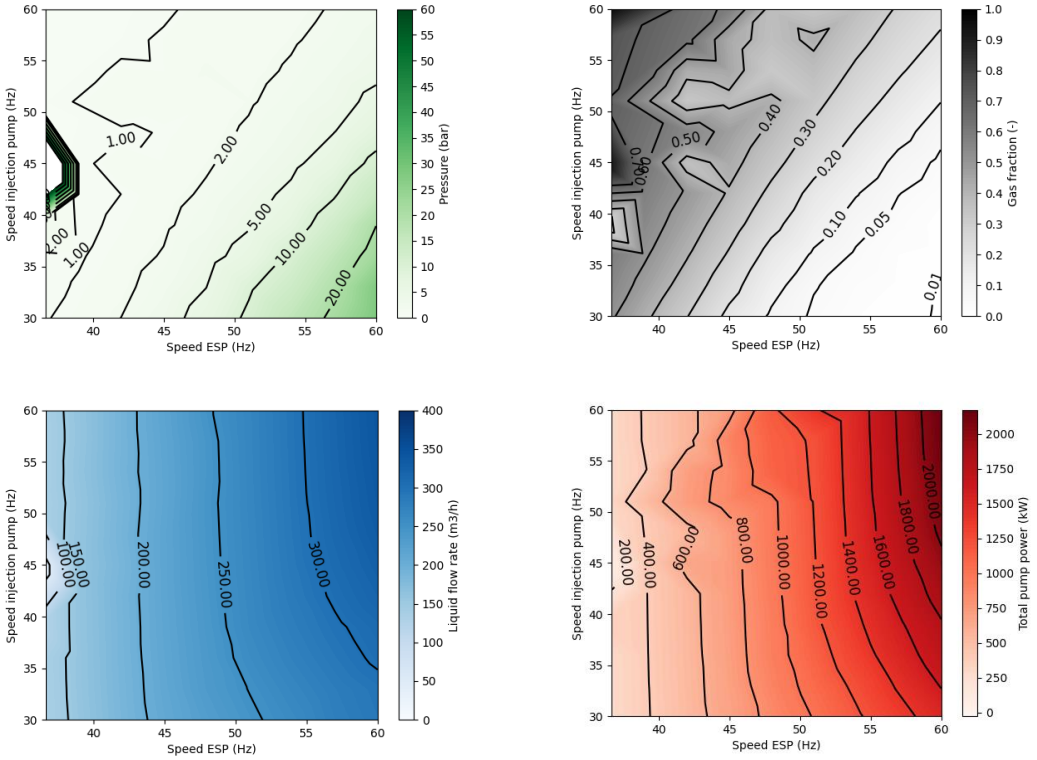

Figure 19: Contour plots of the pressure upstream of the injection pump (top-left), the maximum gas fraction at the topside facilities (top-right), the liquid flow rate (bottom-left) and the total pump power (bottom-right) for an GLR of 1.0 Nm^3/m^3.

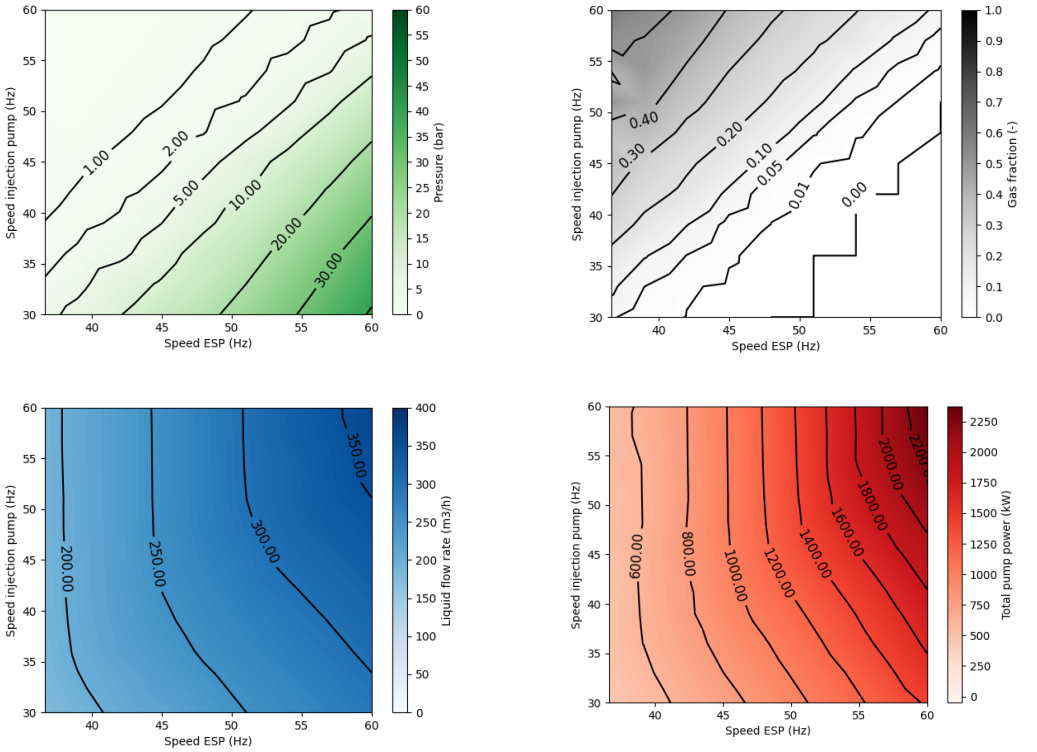

Figure 20: Contour plots of the pressure upstream of the injection pump (top-left), the maximum gas fraction at the topside facilities (top-right), the liquid flow rate (bottom-left) and the total pump power (bottom-right) for the Middenmeer bring with a GLR of 0.33 Nm^3/m^3.

Finally, the effect of the gas composition is investigated in Figure 21. The simulation is the same as the base case, with the exception of the gas composition. In the Heemskerk brine, normally 57 mol % of the gas is methane and 26 mol % of the gas is CO_2. In the contours in Figure 21 this is exactly reversed. As can be observed in Figure 2 and Figure 3 the bubble point pressure of CO_2 is lower than that of methane. As a result, there is a somewhat larger operational range for which the gas volume fraction is 0 in Figure 21 compared to Figure 17. However, in this particular example the pump speeds at which a gas fraction of 0.01 is obtained are almost the same for both gas compositions. In general though, a larger CO_2 fraction typically is helpful in reducing the required topside pressure.

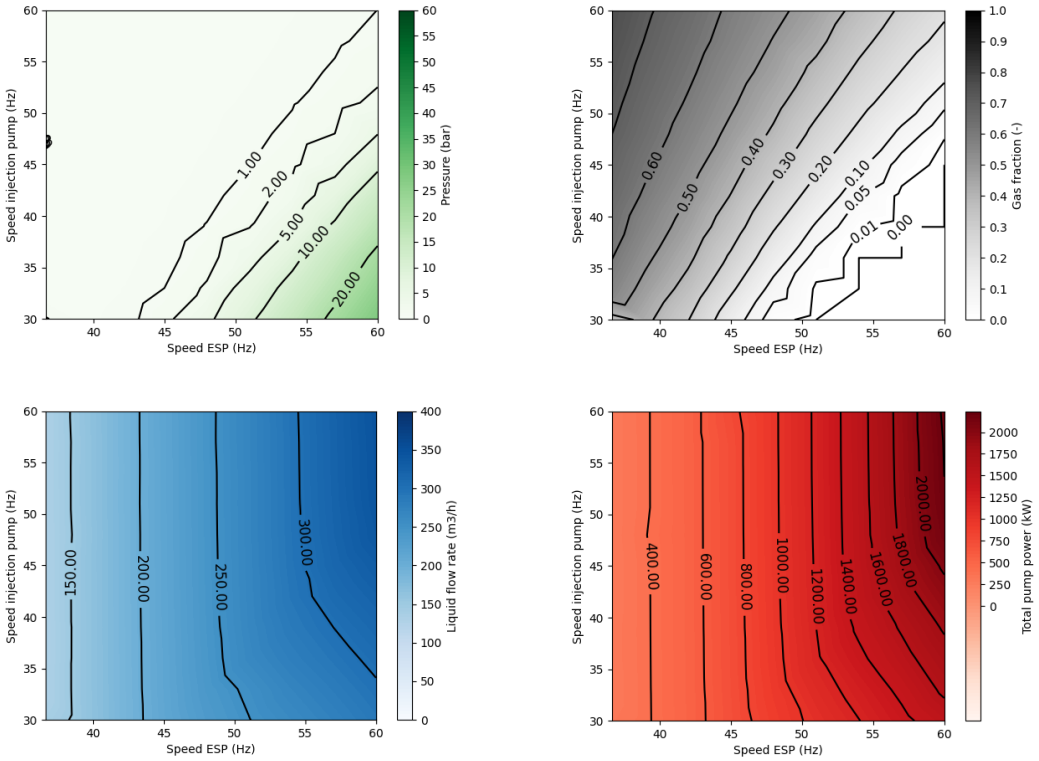

Figure 21: Contour plots of the pressure upstream of the injection pump (top-left), the maximum gas fraction at the topside facilities (top-right), the liquid flow rate (bottom-left) and the total pump power (bottom-right) for the base case in which the fractions of methane and CO_2 in the gas are interchanged.

To elaborate the examples further, in Table 4 the range of flow rates that is possible for the 5 cases at a gas volume fraction of 0.01 is presented, taking into account the current configuration of pumps in the system. In all cases a flow rate of 290 m^3/h is possible so that will be used as an example in the next calculations. In this system the requirements on the ESP are much higher than on the injection pump. It is therefore the strain on the ESP that determines how flexible the system is: lower brine densities, higher reservoir pressures and lower methane fractions all decrease the required pressure increase by the ESP and therefore allow for a larger range in possible liquid flow rates.

Table 4: Possible flow rates at a gas fraction of 0.01 for the five example cases.

Case	**Possible liquid flow rates (m^3/h) at an allowed topside gas fraction of 0.01**
Base case	226.2 to 335.1
High reservoir pressure	208.7 to 367.9
GLR* of 1 Nm^3/m^3	287.5 to 295.7
Middenmeer brine	205.1 to 357.8
Higher CO_2 fraction in the gas	241.8 to 337.8

* GLR: Liquid Gas Ratio

In Table 5 the power consumption of the five different cases to reach a flow rate of 290 m^3/h is presented. Since the efficiency of the injection pump (70%) is greater than the efficiency of the ESP (55%), the total power consumption is higher when the pressure increase from the ESP is higher. Overall, the required power does not change very much between cases. However, for the high GLR case the injection pump is not required anymore. If the gas fraction would be even higher the required topside pressure would also increase, and then it would be required to choke the injection well in order to maintain this flow rate. Systems that combine a high minimum topside pressure with a relatively easy injection (due to a large reservoir injectivity and/or a high brine density) need to be operated at a high flow rate, or the pressure needs to be dissipated at a valve which leads to a lower energy efficiency.

Table 5: The power requirement of the two pumps to achieve a flow rate of 290 m^3/h for each of the five systems.

Case	**Power ESP (kW)**	**Power Injection pump (kW)**	**Total power (MW)**	**Minimum topside pressure (bara)**
Base case	1,326	184	1.51	7.8
High reservoir pressure	974	413	1.39	6.9
GLR of 1 Nm^3/m^3	1,553	0	1.55	25.2
Middenmeer brine	1,007	330	1.34	6.8
Higher CO_2 fraction	1,289	213	1.50	6.1

To compare the energy use with the case with a separator, a slightly different system is simulated. In this system, the pressure at the topside of the production well is set to 1 bara (i.e. the pressure in the separator). The injection pump is then moved to just downstream of this separator, after which the fluid moves through the filters and the heat exchangers. This leads to the power requirements summarized in Table 6. These results show that the required power increase of keeping the system under pressure is relatively low.

Table 6: Power requirements for a system with a separator at the top of the production well.

Case	Power ESP (kW)	Power Injection pump (kW)	Total power (MW)	Difference with keeping under pressure (%)
Base case	1,067	291	1.36	-9.9%
High reservoir pressure	773	587	1.36	-2.2%
GLR of 1 Nm^3/m^3	1,065	292	1.36	-12.3%
Middenmeer brine	801	431	1.23	-8.2%
Higher CO_2 fraction	1,068	291	1.36	-9.3%

2.3.2 The pH in the different injection scenarios

Keeping the CO_2 in the system can potentially lead to a change in the pH in the injection well. This is illustrated for the example cases in Figure 22. The figures were created by calculating the pressure and temperature along the wells in OLGA, and then calculating the pH at those pressures and temperatures in Preeqc. The images show that degassing does lead to an increase of the pH by about 0.2 points. However, even without degassing the pH is slightly higher in the injection well compared to the production well. This is due the cooling of the brine, since pH increases with decreasing temperature. As CO_2 corrosion increases with decreasing pH and with increasing temperature (see e.g. Konovalova (2021) and Prawoto et al. (2009)), the corrosion in the production well will still be worse than in the injection well. If the wells are designed the same, no adjustments to the injection well are required to allow the system to be operated without a separator. Since the pH in the reservoir will change less when keeping the system under pressure, no effects are expected in the reservoir as a result of the gas fraction. The injection of cooled brine can induce changes in the reservoir because the temperature change disturbs the chemical equilibrium, but this is out of scope of the current study.

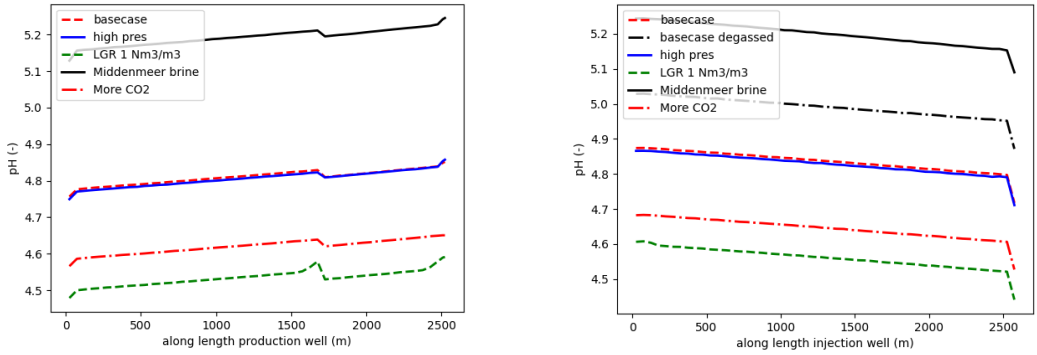

Figure 22: The pH of the brine in the production well (left) and in the injection well (right) for the various cases considered.

2.3.3 The effect on the OPEX and the Coefficient of Performance

The change in OPEX is mainly due to the change in the usage of electricity. Potentially, a change in OPEX is due to a different frequency of the replacement of ESPs or in the higher cost of a replacement ESP. However, in this section this is not taken into account. ESPs are covered in more detail in section 2.5.

The difference in power consumption in the considered cases is between 0.15 and 0.3 MW. Considering an electricity cost of 0.10 €/kWh this leads to an additional cost of 15 to 30 €/h. Assuming 6,000 hours of operation per year, this is 90 to 180k€/y.

To calculate the coefficient of performance, two assumptions are made: (1) all energy usage in the geothermal system is through the two pumps, (2) the output of the system equals the heat extracted from the brine in the heat exchanger. The produced heat of the Heemskerk brine is approximately equal to:

$$H = Q_l \cdot \rho_l c_P (T_h - T_l) \approx 18.6MW$$

In this equation Q_l is the liquid flow rate (in m^3/s), ρ_l is the liquid density, equal to about 1150 kg/m^3 for the Heemskerk brine, c_P is the specific heat, equal to about 3.35 kJ/kgK. The temperature difference is 60°C. For the cases with the Middenmeer brine the ρ_l is lower (1090 kg/m^3) and the c_P is higher (3.51 kJ/kgK). However, these opposite differences result in almost the same amount of produced heat. The COP for the five systems, under pressure and with a separator, are shown in Table 7.

Table 7: Coefficients of performance for both the systems under pressure and the systems with a separator

Case	COP under pressure	COP with separator
Base case	12.3	13.7
High reservoir pressure	13.4	13.7
GLR of 1 Nm^3/m^3	12.0	13.7
Middenmeer brine	13.8	15.1
Higher CO_2 fraction	12.4	13.7

Overall, these results show that the required power to keep the system under pressure requires a modest increase in the power, leading to a decrease of the COP from about 14 to about 13. Of the factors considered here the GLR has the largest effect on the additional power required: keeping the system under pressure is significantly more affordable for a GLR of 0.33 Nm^3/m^3 than for a GLR of 1.0 Nm^3/m^3.

2.3.4 Changes to the topside facilities

All pressurized facilities in the European Union are subject to the Pressure Equipment Directive (PED). In the PED the European rules with respect to pressure vessels and pipelines are specified. For pressures below 0.5 barg the legislation does not apply. For larger pressures there are two main categories:

- Gases and liquids with a vapour pressure above 0.5 barg
- Liquids with a vapour pressure below 0.5 barg

With a separator at atmospheric pressure it is in principle possible to end up in the second of these categories, while keeping everything under pressure always leads to the first of these categories.

Apart from the directive, the topside equipment needs to be able to withstand the larger pressure. It is difficult to determine exactly what the additional cost of the more pressure-resistant equipment is. In the thesis of de Wildt, (2020) this cost is estimated at €30.000,- per bar. Furthermore, when the pressure at the topside is high (for instance at high GLR) an injection control valve is required. The cost of such a valve is about €100.000,-. Next to these expenses, the power requirement of the ESP is larger when the topside needs to be pressurised. More information on the ESP is given in section 2.5.

2.4 Notes on start-up and shut-in of the well and topside design

When shutting down the well in OLGA, using the system presented in Figure 12, a vacuum will appear at the topside (i.e. the reservoir pressure is insufficient to keep the well completely filled with brine up to the surface facilities, causing the brine to flow back into the reservoir and thereby creating a void (= vacuum) at the shut-in valve). To avoid the void from emerging, there should be a way to keep the pressure above or at atmospheric pressure. If the pressure during a shutin at the topside will be atmospheric there will be a significant topside gas fraction. This could lead to a gas lock if the injection pump is started immediately. The ESP is sufficient to get the topside pressure high enough for a low gas fraction < 0.01. Therefore, the ESP should be started first, and the injection pump should initially be bypassed. Only after the pressure at the topside has been increased sufficiently to reduce the gas fraction to a few percent, the injection pump can be started to increase the flow rate.

The separator does not only separate the gas from the liquid, but also catches a lot of sand that is produced. Furthermore, it can act as a buffer between the ESP and the filters. When removing the separator, the produced sand might clog the filters very rapidly. If this happens it might be worthwhile to include a sand trap in the topside design to capture most of the sand before it can clog the filters. Alternatively an alternate completion design can be creased with improved downhole sand control. If some buffer volume between the ESP and the filter is required, for instance to limit the pressure fluctuations reaching the filter, a bladder-type pressure tank can be an option.

2.5 The impact of higher surface pressure on the ESP

This section shortly summarizes the potential impact of the high pressure operation of geothermal systems on the performance and reliability of the ESP. High pressure ESPs have already been seen in the oil and gas industry, but those ESPs are often set at a larger depth. Thus, we would like to review the potential risks in deploying ESPs at a higher surface pressure but at a shallower depth. A common reason for installing a geothermal ESP at shallower depths are (i) to minimize power losses in cables, (ii) to reduce the pressure drop in the tubing between the ESP and the surface, and (iii) to manage the required head with a lower number of stages and less costly inspection and pulling up.

With respect to the allowed gas fraction in the ESP, the literature (see Figure 14) indicates that a gas volume fraction of 1% should not significantly affect the ESP performance, especially in the case of radial stages. Newly developed ESPs can handle gas up to volume fractions of 30% using high volume stages (stage opens up). In such designs, vane openings are wide and there are balance holes which can handle a high volume of gas. Thus, some optimizations in terms of surface pressure and performance of the system are required.

In terms of the impact of high surface pressures on ESP performance, no issue is foreseen apart from a higher power consumption required for the ESP to operate. The main consideration is in the mechanical design review which needs to be performed. Depending on the pressure ratings, a bigger shaft might be required to handle the shaft loading caused by a higher surface pressure. Housing design needs to be checked and reviewed too. In case of design and selection of a new ESP, the number of stages can be optimized as the stage number is determined based on TDH (total dynamic head) and this can allow the ESP to deliver the required head at a lower frequency for a higher number of stages.

The study performed in this report to increase the surface pressure in a system was done with a ESP which was not designed to handle high surface pressures. The following considerations were

suggested for the design review for an ESP that can handle higher surface pressure (surface pressure increased from 6 bars to 30 bars):

- Shaft load was exceeded: decreasing the number of stage could reduce the shaft load but it will increase the frequency and potential wear and tear of the ESP. So, it is suggested that the materials need to be changed.
- Pump Housing and seal shaft (increased to 98%) needed to be reviewed. This is part of the design review to look at pressure differences resulted from the required well production, water level, productivity, setting depth and back pressure.
- The thrust capacity was exceeded
- Motor design was capable of handling the higher surface pressure

Thus, from the considerations above it can be seen that a new design of ESP with a correct number of stages and compatible materials can handle the high surface pressure conditions. Apart from the design considerations, operation of these systems and potential safety risks should be thoroughly evaluated. As an example, potential dead head scenarios such as clogged valves need to be considered for the pressure containment. Consideration such as multiple valves and by-passes are required in stages to ensure the safety of the process.

2.6 Rough cost estimate of keeping the system under pressure

In order to investigate whether keeping the system under pressure is worthwhile, the costs and revenues of keeping the system under pressure are compared with using a CHP (combined heat and power plant). For this comparison, the base case (GLR of 0.33 Nm^3/m^3) and the 1 Nm^3/m^3 cases will be considered. Note that this is a very rough cost estimate, using data obtained by de Wildt (2020). Note that only that part of the cost related to handling greenhouse gasses will be considered here: the overall cost and revenue of the geothermal well are out of scope. Furthermore, a constant flow over 6000 hours per year of 290 m^3/h is assumed, and all components are designed for that flow rate.

The financial consequences of keeping the system under pressure versus using a CHP can be split into two parts: (1) the lost revenue from electricity and heat and the cost of emission of the CO_2 and (2) the CAPEX and OPEX of the CHP and the modifications of keeping the system under pressure. The first part is summarized in Table 8. The table shows that the revenue of the electricity and heat at the assumed prices exceeds the cost of the CO_2 emission.

The second part of the financial comparison concerns the additional CAPEX and OPEX of either running the CHP or of running the system under pressure. Note that these costs are very uncertain and the comparison here is only made to give the reader an idea of what to expect. When actually making the decision on how to operate a geothermal well, this analysis should be redone more thoroughly. An overview of the CAPEX and OPEX is presented in Table 9. The results show that the OPEX and the CAPEX of keeping the system under pressure are higher than for the CHP. Since the differences are relatively small, much depends on the CO_2 emission price, and whether subsidies are available. In the CAPEX calculations the deprecation period of the system is taken to be 30 years, and an interest rate of 8% is assumed. For the annual CAPEX calculation, the equation from Appendix C is used.

Table 8: Overview of the revenues coming from burning greenhouse gasses in a CHP, and the costs of the emission of the CO_2. The price of the methane and electricity is estimated from the 2020 and 2021 data from CBS (2022).

Case	Base case	GLR of 1 Nm^3/m^3
Flow (m3/h)	290	290
Annual gas volume (Nm^3/y)	$5.74 \cdot 10^5$	$1.74 \cdot 10^6$
Mol % CO_2 in gas	25.7	25.7
Mol % CH_4 in gas	57.2	57.2
Mol % N_2 in gas	10.6	10.6
Mass CO_2 in gas (ton/y)	289	877
Mass CH_4 in gas (ton/y)	235	713
Lower heating value methane (MJ/kg)	50	50
Heat of Combustion CH_4 (TJ)	11.8	35.6
Efficiency conversion to electricity (%)	30.8	30.8
Efficiency conversion to heat (%)	47.5	47.5
Electricity price (€/kWh)	0.1	0.1
Heat price (€/GJ)	4	4
CO2 emission cost (€/ton)	80	80
Revenue from electricity (€/y)	101,000	305,000
Revenue from heat (€/y)	22,300	67,700
CO_2 emission (ton/y)	943	2857
Cost CO_2 emission (€/y)	74,800	226,000

Table 9: Estimate of the OPEX and CAPEX of keeping the system under pressure or using a CHP. CAPEX data is taken from de Wildt (2020).

Case	Base case	LGR of 1 Nm^3/m^3
System lifetime (y)	30	30
CAPEX injection valve (€)	0 (not required)	100,000
CAPEX under pressure (€/bar)	30,000	30,000
Topside pressure (barg)	7.6	25.1
CAPEX under pressure (€)	228,000	853,000
Annual equivalent CAPEX under pressure (€) 30 years, 8% interest	**20,300**	75,800
Electricity usage under pressure (MW)	0.15	0.19
Electricity cost under pressure (€)	90,000	114,000
OPEX under pressure (€) includes 30% of annual CAPEX and electricity	**96,090**	136,740
Annual OPEX+CAPEX Under pressure (€)	110,390	212,540
CAPEX CHP (€/kW electric)	2500	2500
CAPEX CHP (€)	419,000	1,270,000
Annual equivalent CAPEX CHP (€) 30 years, 8% interest	37,200	113,000
OPEX CHP (€)	30% of annual CAPEX 11,200	30% of annual CAPEX 33,900
Annual OPEX+CAPEX CHP (€)	48,400	147,000

2.7 Summary

In this chapter the option to keep the geothermal system under pressure to avoid degassing entirely and thereby avoid the emission of greenhouse gases was studied. If a relatively small fraction (up to 1%) of undissolved gas is allowed, the required pressure at the topside is not so large. The gas fraction as a function of pressure has a long tail, so completely avoiding gas in the topside requires a significantly higher pressure.

For small gas fractions of 0.33 Nm^3/m^3 the required topside pressure of at most 9 bar probably does not require significant changes to the topside facilities (please note that this value depends on the careful characterization of the geothermal brine and gas and measuring the bubble point of the solution). Only a relatively small increase in the power cost is required to keep the system under pressure: the ESP is typically less efficient than the injection pump. At the larger gas fraction of 1 Nm^3/m^3 the required topside pressure is significantly larger (26 bar). This will require more changes in the topside design, including a design review of the ESP. In this report, there is not yet an accurate cost estimate of the required change to the topside to keep the system under pressure.

Overall, keeping the system under pressure requires higher pressures, and therefore is more costly, when the gas fraction is high and the gas contains a lot of methane (which is less soluble in water than nitrogen and carbon dioxide). Furthermore, there is a lot of potential for using the methane – by burning it to obtain additional electricity and heat – or for selling it to the marked. Therefore, in the next chapters two alternatives are explored in which the methane is either used or sold.

3 CHP combined with CO_2 storage

3.1 Introduction

In the work by Ros & Monteiro (2021), the techno-economic feasibility of a carbon capture system for a geothermal well was evaluated. Such a system would be required in order to capture the CO_2 emitted by a combined heat and power (CHP) plant that would use the methane coming from the geothermal brine as fuel.
The authors used two example cases to assess the feasibility: a single well or a cluster of ten geothermal wells of which the gas is burned in a single CHP. For each well, 1 Nm^3 gas per m^3 geothermal brine is produced. The composition of the gas is specified in Table 10. Each well produced 200 m^3/h hot brine for 8760 operational hours per year. The gas was burned in a CHP and the CO_2 from the flue gas was separated (using amine-based technology) and injected in the injection well. In practice, geothermal wells have around 6000 operational hours per year and their results have been updated in Figure 23 to reflect this (note that the estimates by Ros & Monteiro of the CAPEX of the capturing plant is much lower than estimated via the model given in appendix C, making their business case more positive). From these results, it was concluded that CO_2 capture for a single well is not financially feasible and that a relatively large number of wells are required to make capture financially attractive.

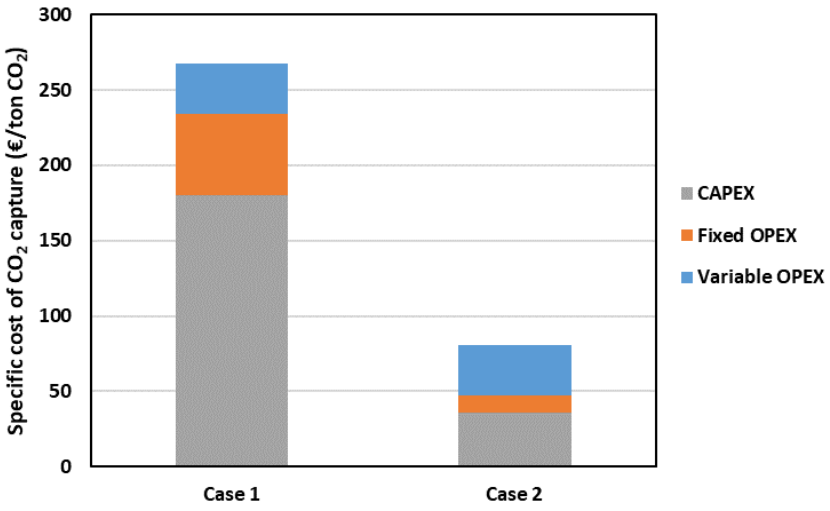

Figure 23: Cost of CO_2 capture per ton as calculated by Ros & Monteiro (2021), corrected for total operational hours per year. Case 1 considers a single geothermal doublet, case 2 considers 10 geothermal doublets combined.

Here, the analysis of Ros & Monteiro (2021) is extended in order to determine whether it can, under certain circumstances, be made feasible to apply carbon capture to a smaller number of wells, e.g., by additionally capturing the CO_2 from the 'bijstook' in the winter season (Q1) to make carbon capture financially more attractive. Details on the techno-economic model of the amine-based carbon capture are given in appendix C. In Figure 24 a schematic of the system that is analyzed in this chapter is presented. Heat is produced from two geothermal doublets. The greenhouse gasses from the doublet are burned in a CHP, from which electricity and gas is produced. The flue gas is then lead to an amine carbon capture facility. Part of the heat and electricity generated by the CHP is used to drive this carbon capture facility. The remaining heat and electricity can be used elsewhere or sold. In each scenario presented in this chapter, a baseline calculation is performed for a system without carbon capture, i.e. where the flue gas is directly released into atmosphere.

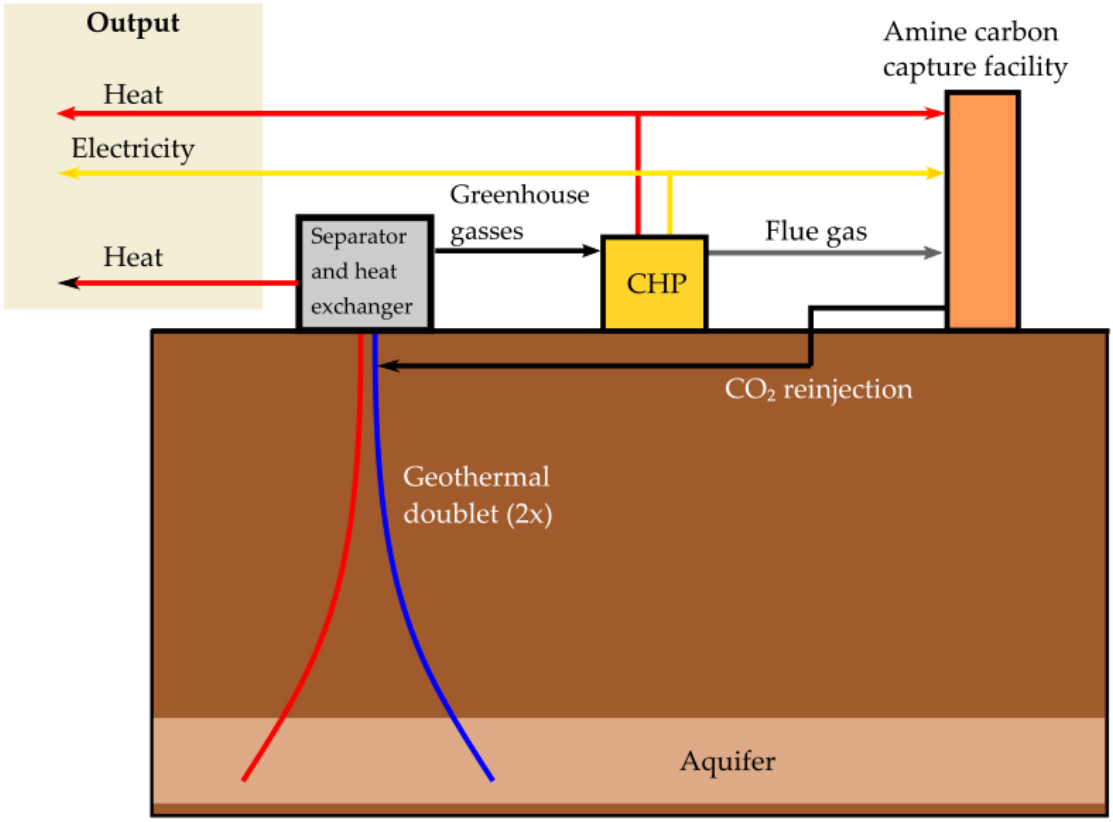

Figure 24: Schematic of the system considered in this chapter. The greenhouse gasses are burned in a CHP (or a boiler in scenario 4). Then carbon capture is performed on the flue gas and the CO_2 is reinjected into the well. Note that in each scenario, both the case with and without carbon capture is considered.

In geothermal wells often additional gas is burned in the winter season (Q1) due to a higher heat demand. This is also called 'bijstook'. As an example, in a paper by Bloemendal (2021) it is indicated that 65 TJ of energy from 'bijstook' is required based on an annual generation of the geothermal well of ~235 TJ, i.e. bijstook is about 25% of the energy from the geothermal well. In the current assessment this percentage is also used, and it is assumed that this energy is required in the winter season for 3 months (i.e. during these three months the heating power of the 'bijstook' equals that of the geothermal well, thereby doubling the heating power in winter compared to the other seasons (Q2-4)).

Several scenarios, all for 2 geothermal doublets, are assessed and compared:

1. 2 Constant flow. All gas is burned in a CHP. During the winter season additional heat is purchased to meet the heat demand (i.e. no 'bijstook')
2. Constant flow during spring, summer and autumn (Q2-4). In the winter season (Q1) the heat production by the geothermal well is doubled to meet the heat demand (i.e. no 'bijstook'). All gas is burned in a CHP.
3. Constant flow. In the winter season (Q1) 'bijstook' is used to compensate for the required additional heat in Q1 (using gas from the grid). All gas is burned in a CHP.
4. Constant flow. In the winter season (Q1) 'bijstook' is used to compensate for the required additional heat (using gas from the grid). All gas is burned in a boiler.

These scenarios are summarized in Figure 25, which shows the hear demand profile, and the way in which the demand is met.

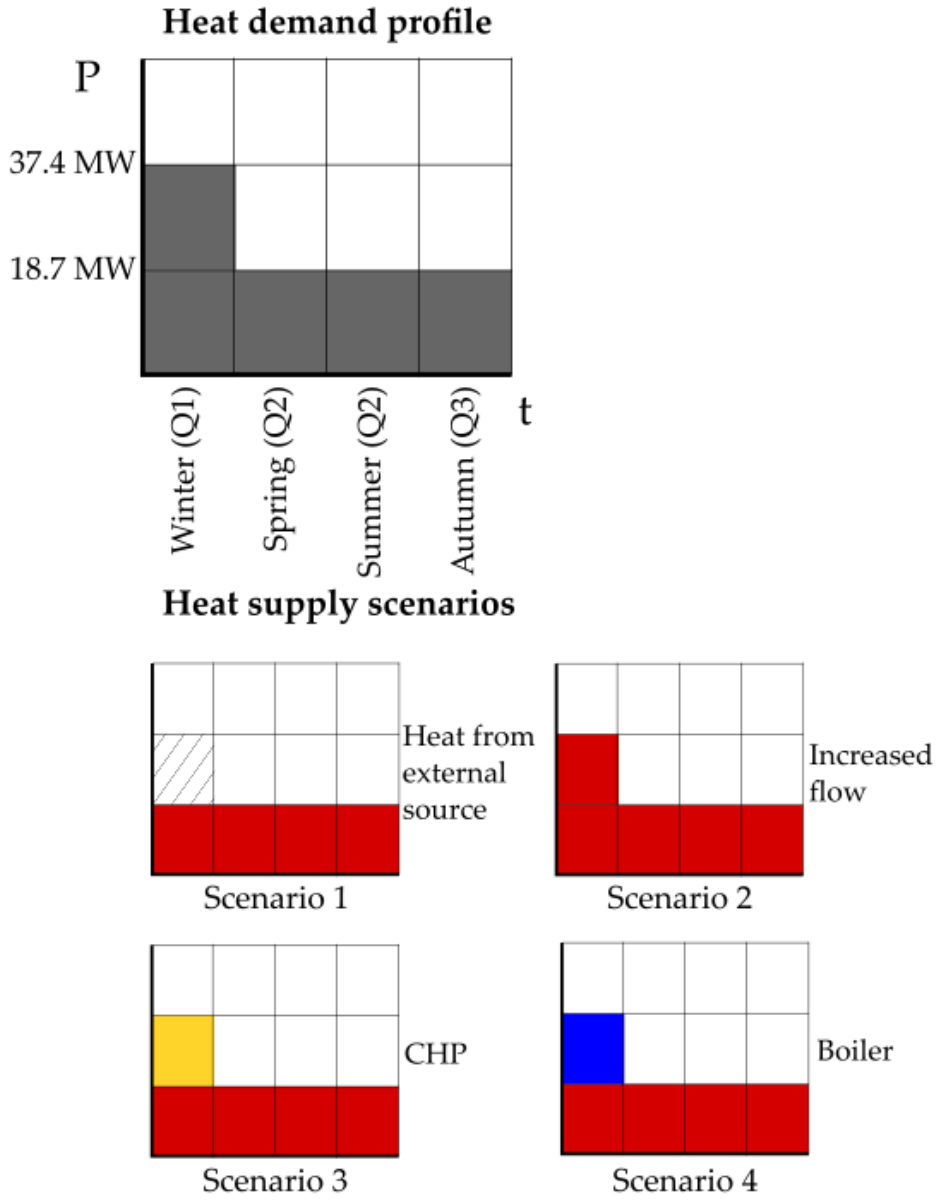

Figure 25: Schematic of the heat demand (top) and the way in which this heat demand is met in the 4 considered scenarios.

To highlight the impact of carbon capture, all scenarios are computed without capture (scenarios 1a, 2a, 3a and 4a) and with carbon capture (scenarios 1b, 2b, 3b and 4b). The assessment of the various scenarios addresses energy consumption, CO_2 emissions, pH, and a rough economic evaluation. The economic evaluation has been done on a limited number of relevant aspects, using rough estimates. Therefore, it can be used only to compare the results within this chapter.

A best case scenario for carbon capture is made by assuming the geothermal well to have a very large GLR of 1.5 Nm^3/m^3 to attempt improving the economics-of-scale. The gas composition is specified in Table 10. Other parameters used in this chapter are summarized in Table 11.

Table 10: Gas specification assumed in this chapter.

Component	**Mol %**
CH_4	89.36
CO_2	8.96
N_2	1.71

Table 11: Parameters common to all cases in this chapter.

Quantity	**Value**
ΔT (heat exchanger)	40°C
Production rate	200 m^3/h per well, 2 wells
Brine heat capacity	4.2 kJ/kg K
Yearly operational hours	6000 h
Gas to liquid ratio	1.5 Nm^3/m^3
CHP heat recovery (%)	47.5
CHP electricity recovery (%)	30.8

From these inputs, the additional quantities presented in Table 12 can be calculated.

Table 12: Quantities calculated from the specified parameters.

Instantaneous heat supply base rate (MW)	18.7
Cumulative hear supply at base rate assuming 6000 operational hours annually (TJ)	400
Gas volume (Nm^3/h)	600
Flue gas volume (kNm^3/h)	14.2
CO_2 fraction flue gas (mol %)	4.2[(6)]
Lower Heating Value (LHV) (MJ/kg)	50
Density CH_4 (kg/Nm^3)	0.717
Combustion heat at base rate (MW)	5.34
CO_2 production (kton/y)	7.1
CO_2 production intensity (kg CO_2/MWh)	220
CHP electricity production (MW)	1.64
CHP heat production (MW)	2.54

Note that these scenarios may involve the injection of CO_2 into the geothermal reservoir that does not come from the reservoir itself, i.e. as a product of the combustion of the geothermal gas or gas taken from the grid. This could lead to increases in the reservoir pressure. Also, additional permitting might be required.

3.2 Scenario 1

In scenario 1a the CO_2 is not captured, hence a total of 7.1 kton CO_2 is emitted annually. In Q2-4 a total of 2.54 MW_{th} of heat produced by the CHP can be utilised (i.e. ~41 TJ over a period of 4500 h). In Q1 the heat demand increases to 37.4 MW_{th}, thus a total of 16.1 MW_{th} heat (= 37.4 – 18.7 – 2.54) needs to be purchased (i.e. ~87 TJ over a period of 1500 h). The electricity produced by the CHP can always be sold. The pH of the geothermal brine will increase, since CO_2 is removed from the brine and not injected back in the geothermal brine. This may have a positive effect on the corrosion risk, but an adverse effect on the scaling risk in view of calcium carbonate scaling. Table 13 shows some estimated costs and gains relevant for scenario 1a. The sales of electricity seem to balance the cost for the CHP and CO_2 emissions roughly.

[6] This is a typical number for the flue gas composition of a CHP (ref. Ros & Monteiro (2021)). Note that when the CO_2 fraction in the geothermal gas increases at the cost of CH_4, the fuel/air ratio does not change, hence the total flue gas flow rate remains the same.
[7] Annual Cost CHP = Equivalent Annual CAPEX (using CAPEX of CHP = 2.5 M€/MW_e, 30 y lifetime, 8% interest) plus OPEX (taken as 10% of Equivalent Annual CAPEX).

Table 13: Overview of costs for scenario 1a

	Cost	Amount	Total
CO_2 emission	- 80 €/ton	7.1 kton/y	-565 k€/y
Annual Cost CHP [7]			-475 k€/y
Sales of electricity	+ 0.1 €/kWh	9.9 GWh/y	987 k€/y
Sales of heat	+ 4 €/GJ	458 TJ/y	1832 k€/y

In scenario 1b a CO_2 capture plant is installed. Using a 90% CO_2 capture rate, a total of 0.54 kNm^3/h is captured, which is equal to 1.06 ton/h or 6.35 kton/y. The remainder of the CO_2 is emitted (i.e. 0.71 kton/y). The plant further requires ~1.15 MW_{th} heat (3.9 GJ_{th}/ton CO_2) and ~320 kW_e electricity (300 kWh_e/ton CO_2), see appendix C, which is equal to about 45% and 20% of the heat and electricity generated by the CHP, respectively. In summer the remainder of the heat (1.4 MW_{th}, or 23 TJ over a period of 4500 h) is sold, but in winter it is used for the increased heat demand. The excess electricity (1.3 MW_e) can always be sold.

In the winter season heat needs to be purchased in order to meet the winter demand of 37.4 MW_{th}. In this period, the geothermal well supplies 18.7 MW_{th} and the CHP supplies 2.54 MW_{th} of heat. Taking into account the requirements for the capturing process (1.15 MW_{th}), an additional 17.3 MW_{th} needs to be purchased (i.e. ~ 93 TJ over a period of 1500 h).
By burning the geothermal gases and injecting the captured CO_2 back into the injection brine stream, the CO_2 content in the brine increases from 54 Nm^3/h (present in the brine in the production well) to 0.54 kNm^3/h (i.e. an increase of a factor of ~10). Injecting this CO_2 into the geothermal brine causes the pH to drop from ~4.3 in the injection well to ~3.8 (see appendix D)(both for summer and winter).
For the carbon capture plant dimension to capture 1.06 ton/h, a CAPEX of ~13.5 M€ is involved (see appendix B). This corresponds to an equivalent annual CAPEX of ~1.2 M€/y (based on a 30 years lifetime and 8% interest rate). Using a CO_2 capture rate of 6.35 kton/y, this results in an effective CAPEX per captured CO_2 of ~190 €/ton CO_2.
The fixed OPEX [8] of the carbon capture plant is about 30% of the equivalent annual CAPEX or 360 k€/y (or ~57 €/ton CO_2) and the variable OPEX [3] is 45.6 €/ton CO_2 (see appendix C). This brings the total carbon capture cost to ~290 €/ton CO_2 or ~1.85 M€/y. Table 14 shows some estimated costs and gains relevant for scenario 1b.

Table 14: Overview of costs for scenario 1b

	Cost	Amount	Total
CO_2 emission	- 80 €/ton	0.7 kton/y	-56 k€/y
CO_2 capture	- 290 €/ton	6.4 kton/y	-1852 k€/y
Annual Cost CHP [7]			-475 k€/y
Sales of electricity	+ 0.1 €/kWh	8 GWh/y	796 k€/y
Sales of heat	+ 4 €/GJ	439 TJ/y	1758 k€/y

As expected, the CO_2 emissions are much reduced when carbon capture is applied. However, the capturing for scenario 1b is more expensive mainly due to the low volume of the CO_2 flow. Considering the costs and revenues listed in the tables, scenario 1b is ~1.6 M€/y more expensive than scenario 1a.

[7] Annual Cost CHP = Equivalent Annual CAPEX (using CAPEX of CHP = 2.5 M€/MW_e, 30 y lifetime, 8% interest) plus OPEX (taken as 10% of Equivalent Annual CAPEX).

[8] Fixed operating costs are the actual costs associated with operating a property that do not vary in the short term. These costs do not change with a property's occupancy rate. Property insurance is a common example of a fixed operating cost. Variable operating costs do depend on the occupancy rate, i.e. fuel cost (www,realized1031.com).

3.3 Scenario 2

In scenario 2, the additional heat required in winter (18.7 MW for 1500 h, i.e. ~100 TJ) is supplied by the geothermal brine that is producing more heat by increasing the flow to 400 m^3/h per well [(9)]. As a consequence, an additional 1.8 kton of CO_2 is produced during winter.

Scenario 2a and 2b, are very similar to scenario 1a and 1b, respectively. The main results on the emissions and costs are given in Table 15 and Table 16. Here it is noted that the impact of doubling the heat production from the geothermal well on the operational and maintenance costs are not considered here. Also, compared to scenario 1a, the annual costs of the CHP are relatively higher (due to the capacity in Q1), such that the revenues of the sales of electricity is lower than the annual cost of the CHP and CO_2 emissions.

Table 15: Overview of costs for scenario 2a.

	Cost	Amount	Total
CO_2 emission	- 80 €/ton	8.8 kton/y	-706 k€/y
Annual Cost CHP [(7)]			-950 k€/y
Sales of electricity	+ 0.1 €/kWh	12.3 GWh/y	1233 k€/y
Sales of heat	+ 4 €/GJ	574 TJ/y	2290 k€/y

Table 16: Overview of costs for scenario 2b

	Cost	Amount	Total
CO_2 emission	- 80 €/ton	0.88 kton/y	-71 k€/y
CO_2 capture	- 365 €/ton	7.9 kton/y	-2900 k€/y
Annual Cost CHP [(7)]			-950 k€/y
Sales of electricity	+ 0.1 €/kWh	10 GWh/y	995 k€/y
Sales of heat	+ 4 €/GJ	542 TJ/y	2166 k€/y

Compared to scenario 1, in Q1 the impact on the corrosion in the production and injection well may be somewhat higher, since the flow velocity increases by a factor 2 (at similar levels of the pH as in scenario 1). Comparing scenario 1b with 2b the capture costs increases from 290 €/ton CO_2 for scenario 1b to 365 €/ton CO_2 for scenario 2b. This is caused by the fact that in scenario 2b the capture plant is not running at full load in Q2-4, which is not efficient (i.e. the capture plant is over-dimensioned for Q2-4). Considering the costs and revenues listed in the tables, scenario 2b is ~2.6 M€/y more expensive than scenario 2a.

3.4 Scenario 3

In this scenario the increased heat demand in Q1 is supplied by the CHP that is using additional gas from the grid (assumed to have 90 mol% CH_4). Scenario 3a is very similar to scenario 1a. The main results on the emissions and costs are given in Table 17.

Compared to scenarios 1a and 2a, the annual costs of the CHP are relatively much higher (due to the higher capacity in Q1), such that the revenues of the sales of electricity is much lower than the annual

[9]Alternatively the heat production of the geothermal wells can also be increased by decreasing the return temperature, for instance increasing the flow to 300 m3/h and decreasing the return temperature by 14 °C would also double the heat production. This would decrease the positive effects of economics-of-scale of the capture plant, but the difference between the maximum and minimum flue gas flow is reduced, which is more efficient. Overall the total Carbon capture cost is then about 336 €/kg CO_2 and the total gain is about 0.58 M€/y. Note that these low injection temperatures might not be allowed.

cost of the CHP and CO_2 emissions. Considering the costs and revenues listed in the tables, scenario 3a is much more expensive than scenario 1a (~5.5 M€/y), due to the large costs for the CHP and purchasing gas. CO_2 emissions are also much higher than for scenario's 1 and 2.

Table 17: Overview of costs for scenario 3a

	Cost	Amount	Total
CO_2 emission	- 80 €/ton	17.3 kton/y	-1381 k€/y
Annual Cost CHP [7]			-3500 k€/y
Sales of electricity	+ 0.1 €/kWh	25.6 GWh/y	2556 k€/y
Sales of heat	+ 4 €/GJ	545 TJ/y	2180 k€/y
Purchase of gas	- 0.65 €/Nm^3	5.68 kNm^3/y	-3694 k€/y

In scenario 3b a CO_2 capture plant is installed. However, since the amount of CO_2 produced in Q1 is much more than in Q2-4 (>5x), it is not likely that the dynamic range of a CO_2 capture can handle this. Here it is assumed that the carbon capture plant can be operated at 30-100% of its total capacity, and that the CO_2 production in Q2-4 (being 30% of rated capacity) determines the plant size. Using a 90% CO_2 capture rate in Q2-4 the CO_2 captured flow rate is 1.06 ton/h. In Q1, making full use of the assumed dynamic range, the capture plant captures 3.53 ton/h (= 1.06 / 0.3). In this period, the plant requires 3.8 MW_{th} heat and 1.06 MW_e electricity.

The total heat demand in Q1 is then 41.2 MW_{th} (= 37.4 + 3.8), which is supplied by the geothermal brine (18.7 MW_{th}), usage of the geothermal gas in the CHP (2.54 MW_{th}) and additional gas from the grid combusted in the CHP (~20 MW_{th}). The 20 MW_{th} is covered by combusting 4.7 kNm^3/h gas from the grid. This results in a total CO_2 production of 19.7 kton/y, of which 10.1 kton/y is captured and the remaining 9.6 kton/y is emitted.
By burning the geothermal gases and gas from the grid, the CO_2 stream that is to be injected back into the brine increases from 54 Nm^3/h (normally present in the brine) to 0.54 kNm^3/h in Q2-4 (i.e. an increase of a factor ~10) and to 1.8 kNm^3/h in Q1 (i.e. an increase of a factor of ~33). This causes the pH to drop from ~4.3 in the production well to ~3.8 in Q2-4 and to ~3.5 in Q1 in the injection well. The main results on the emissions and costs for scenario 3b are given in Table 18.

Table 18: Overview of costs for scenario 3b

	Cost	Amount	Total
CO_2 emission	- 80 €/ton	9.6 kton/y	-770 k€/y
CO_2 capture	- 406 €/ton	10.1 kton/y	-4088 k€/y
Annual Cost CHP [7]			-4200 k€/y
Sales of electricity	+ 0.1 €/kWh	26.3 GWh/y	2626 k€/y
Sales of heat	+ 4 €/GJ	527 TJ/y	2106 k€/y
Purchase of gas	- 0.65 €/Nm3	7.03 kNm^3/y	-4570 k€/y

As the variation in capture capacity between Q1 and Q2-4 is larger for scenario 3b than for scenario 2b and 1b, the capture cost also increases due to the larger inefficient operations. This also holds for the CHP. Also, since the variation in CO_2 flow cannot be handled by the capturing plant, the CO_2 emissions are still rather high. Considering the costs and revenues listed in the tables, scenario 3b is ~5 M€/y more expensive than scenario 3a.

3.5 Scenario 4

In this scenario a boiler is used instead of a CHP to burn the geothermal gas and, in Q1, the additional gas from the grid. Assuming a heat recovery of 90% for a boiler, less gas is required to meet the heat demand, but the electricity generation is zero. Burning the geothermal gas in the boiler then generates 4.8 MW_{th}.

Scenario 4a is very similar to scenario 1a, and scenario 4b is very similar to scenario 3b. The main results on the emissions and costs of scenarios 4a and 4b are given in Table 19 and Table 20, respectively. Compared to scenario 3a, the annual costs of the boiler are relatively much smaller than for the CHP. With a much smaller amount of gas required (also resulting in a lower CO_2 emission), the net revenues is more positive for scenario 4a than for 3a (~3.4 M€/y, considering the costs and revenues listed in the tables).

Table 19: Overview of costs for scenario 4a

	Cost	Amount	Total
CO_2 emission	- 80 €/ton	11.7 kton/y	-935 k€/y
Annual Cost boiler [10]			-162 k€/y
Sales of heat	+ 4 €/GJ	582 TJ/y	2327 k€/y
Purchase of gas	- 0.65 €/Nm3	2.58 kNm^3/y	-1675 k€/y

Table 20: Overview of costs for scenario 4b

	Cost	Amount	Total
CO_2 emission	- 80 €/ton	2.9 kton/y	-223 k€/y
CO_2 capture	- 406 €/ton	10.1 kton/y	-4088 k€/y
Annual Cost boiler [10]			-195 k€/y
Sales of heat	+ 4 €/GJ	563 TJ/y	2253 k€/y
Purchase of gas	- 0.65 €/Nm3	3.28 kNm^3/y	-2138 k€/y

Comparing scenario 4b (boiler + capture) with scenario 3b (CHP + capture) the capture costs are the same. However, the annual costs of a boiler are much smaller than for a CHP, and require less gas to meet the demand in Q1 (i.e. also smaller CO_2 emissions and related costs). Therefore, scenario 4 is more attractive than scenario 3. Considering the costs and revenues listed in the tables, scenario 4b is ~4 M€/y more expensive than scenario 4a (with high emissions) and scenario 2b (with low emissions).

3.6 Summary

8 Scenarios have been considered to assess whether a carbon capture process is feasible to deal with the GHG from the geothermal well and optionally the 'bijstook' in winter (Q1) to make use of positive scale-up effects. Scenarios 1a, 2a, 3a and 4a involve those without capturing and scenarios 1b, 2b, 3b and 4b are with capturing. Table 21 compares the total CO_2 production, capture and emissions and associated costs for the various scenario's considered.

[10] Annual Cost boiler = Equivalent Annual CAPEX (using CAPEX of boiler = 75 k€/MW_e, 30 y lifetime, 8% interest) plus OPEX (taken as 10% of Equivalent Annual CAPEX).

Table 21: Overview of the CO_2 production related parameters for the various scenarios over a full year.

Scenario	1a	1b	2a	2b	3a	3b	4a	4b
CO_2 production (kton/y)	7.1	**7.1**	8.8	**8.8**	17.3	**19.7**	11.7	**13.0**
Emission (kton/y)	*7.1*	*0.7*	*8.8*	*0.9*	*17.3*	*9.6*	*11.7*	*2.9*
Capture (kton/y)		*6.4*		*7.9*		*10.1*		*10.1*
CO_2 Capture cost (*€/ton*)		**291.5**		**365.2**		**406.4**		**406.4**
CAPEX		*189.2*		*245.9*		*277.5*		*277.5*
Fixed OPEX		*56.8*		*73.8*		*83.3*		*83.3*
Variable OPEX		*45.6*		*45.6*		*45.6*		*45.6*
CO_2 cost (k€/y)	565	**1909**	706	**2971**	1381	**4859**	935	**4321**
Capture (k€/y)		*1852*		*2901*		*4088*		*4088*
Emission @ 80€/ton (k€/y)	*565*	*56*	*706*	*71*	*1381*	*770*	*935*	*233*

CO_2 emissions are non-zero for all scenario's even when CO_2 capture is considered. This is due to the limited capture efficiency (assumed maximum 90%), and due to the limited dynamic capacity range of the capture plant (i.e. the minimum capacity of the capture plant is assumed to be 30% of its design capacity, and the CO_2 production in Q2-4 is set to this minimum capacity).

For all scenario's with CO_2 capturing, the CO_2 emissions are significantly reduced compared to the scenario's without capturing. The costs involved with the capturing, however, is much larger than the assumed emission costs. The reasons for the high costs are:

- Relatively low volumes of CO_2 that need to be handled.
- Variations of the CO_2-flow-streams cause an over-dimensioning of the capturing plant during low capacity periods. This causes the addition of 'bijstook' in the capturing plant not to provide any positive effects of economics-of-scale: adding 'bijstook' increases the variation in handling capacity.

Using the CHP to burn the geothermal gas does provide electricity which has a higher value than heat. However, when additional gas needs to be purchased from the grid to meet the heat demand, the 'low' heat recovery of a CHP requires a larger amount of gas from the grid to be used. This in turn results in a higher CO_2 production (and consequently emissions). The extra revenues from the electricity production may just balance the costs for the extra gas that needs to be purchased and the CO_2 emission, but the investments for a CHP to deal with the variation in capacity is much larger than for a boiler. In that sense, the use of a boiler to meet the increased heat demand in Q1 is a better choice, having lower CO_2 production and emissions and lower costs.

As CO_2 capturing is very energy consuming, the CO_2 capturing cost will increase with increasing energy prices. Currently an increase in energy prices tends to reduce the global energy usage, which will decrease the global CO_2 emission and, most likely, therefore also the emission costs. It is thus expected that an increase in energy prices will make the capturing process financially even less attractive compared to emissions.

In case the GLR is smaller than the assumed 1.5 Nm^3/m^3, the CO_2 capturing cost per ton CO_2 as well as the overall CO_2 emissions will be higher, making the CO_2 capturing even less attractive.

4 Sell methane and CO_2

In this section, the sales of the methane and the separate capturing of the CO_2 is briefly considered. In these scenarios, the gas from the geothermal well is directly fed to a CO_2 capturing process on-site to separate most of the CO_2 from the formation gas. For this separation an amine-based technology can be used, similar as the CO_2 capturing in chapter 3 (see appendix C for a description). The separation system now can be smaller, as the CO_2-flow is approximately 10x smaller compared to when CH_4 is combusted and CO_2 needs to be separated from the flue stream.

In this chapter, the system in Figure 26 is considered. It contains having two doublets, each producing 200 m^3/h in Q2-4 (4500 h) and 400 m^3/h in Q1 (1500 h), and having a GLR of 1.5 Nm^3/m^3, 1 Nm^3/m3 or 0.33 Nm^3/m3. The gas composition is taken as: 89 mol% CH_4, 9 mol% CO_2, 2 mol% N_2. The amount of CO_2 produced in Q1 by the geothermal well is twice the amount in Q2-4, which is assumed to be possible for handling in a capturing plant.

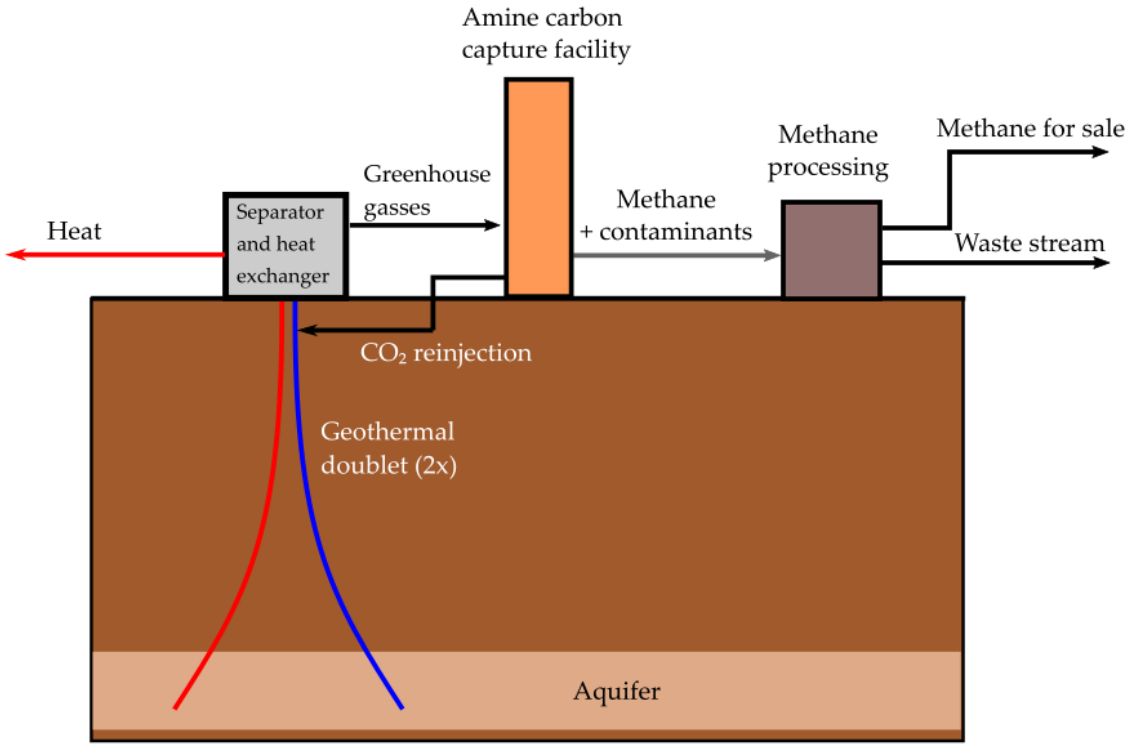

Figure 26: Schematic of the system considered in this chapter. Greenhouse gasses from the geothermal wells are immediately taken to an amine carbon capture facility where the CO_2 is separated from the other components. The CO_2 is reinjected into the geothermal doublets, while the methane is processed and then sold.

For GLR = 1.5 Nm^3/m^3 the well produces 2.9 ton/y CH_4 and 0.8 ton/y CO_2. Using a 90% CO_2 capture rate in Q2-4 the CO_2 captured flow rate is 0.1 ton/h. The plant further requires ~0.1 MW_{th} heat (3.9 GJ_{th}/ton CO_2) and ~22 kW_e electricity (235 kWh_e/ton CO_2), see appendix C. In Q1, the capture plant captures 0.2 ton/h. In this period, the plant requires ~45 kW_e electricity and 0.2 MW_{th} heat. In total 715 ton CO_2 is captured annually, which is injected back into the well. The remaining CO_2 flows with the methane to the grid (~97 mol% CH_4, ~1 mol% CO_2), and GHG emissions at the geothermal site are essentially zero.

The pH of the geothermal brine in the injection well will be roughly equal to that in the production well, since 90% of the CO_2 is injected back. Thus corrosion and scaling risks are expected to be unchanged. Note that in this work the use of the sold methane is not considered. This has to be done in a facility that uses carbon capture in order to actually avoid the bulk of the greenhouse gas emissions and not just emit it elsewhere.

For GLR = 1.5 Nm^3/m^3, the carbon capture plant is dimensioned to capture the flow in Q1 (= 0.1 ton/h), for which a CAPEX of ~4.1 M€ is involved (see appendix C). This corresponds to an equivalent annual CAPEX of ~360 k€/y (based on a 30 years lifetime and 8% interest rate). Using a CO_2 capture rate of 715 ton/y, this results in an effective CAPEX per captured CO_2 of ~500 €/ton CO_2. The fixed OPEX of the carbon capture plant is about 30% of the equivalent annual CAPEX or ~110 k€/y (or ~150 €/ton CO_2) and the variable OPEX is ~39 €/ton CO_2 (see appendix C). This brings the total carbon capture cost to ~700 €/ton CO_2. This corresponds to ~500 k€/y or 0.12 €/Nm^3 CH_4. Note that the components in the gas in the Dutch grid are specified. On the one hand, this is helpful. The gas in the grid often has a higher nitrogen content than the gas in geothermal wells, such that the nitrogen does not need to be separated out of the mixture. However, it does mean that the produced methane needs further processing before it is possible to deliver it to the grid. As a rough estimate, a margin of 50% is added to the costs for methane processing and transport, raising the cost to 0.19 €/Nm^3 CH_4.
Here it is noted that in the current work the most developed technology for CCS is considered, the amine based capture plant. Future developments in e.g. membrane separation, might make it possible to construct smaller and more cost effective plants for these relatively small gas streams.

Table 22 presents key numbers on the separation of CH4/CO2 required for selling CH4 for GLR = 1.5, 1 and 0.33 Nm3/m3.

Table 22: Overview of the CH_4/CO_2 separation related parameters for the various scenarios over a full year.

GLR	1.5 Nm^3/m^3	1 Nm^3/m^3	0.33 Nm^3/m^3
CH_4 produced	4000 kNm^3/y	2700 kNm^3/y	880 kNm^3/y
Annual Separation cost	750 k€/y	560 k€/y	250 k€/y
Separation cost per Nm^3 CH_4	0.19 €/Nm^3	0.21 €/Nm^3	0.29 €/Nm^3
Revenues from CH_4 sales (*)	2615 k€/y	1740 k€/y	575 k€/y
Revenues from sales of heat (**)	2015 k€/y	2015 k€/y	2015 k€/y
Net revenues	3.9 M€/y	3.2 M€/y	2.3 M€/y

(*) at 0.65 €/Nm^3
(**) at 4 €/GJ

With a decrease of GLR the separation cost becomes relatively more expensive (per Nm^3 CH_4), but the overall annual separation costs decrease. A decrease of GLR also decreases the revenues from the sales of CH_4, as well as the net revenues although they seem to stay positive.
In case the CO_2 content increases, the separation will become more expensive and the revenues from sales of CH_4 will decrease. Following a similar approach as above, increasing the CO_2 content to ~30% will make the revenues from CH_4 sales about equal to the separation cost, i.e. this technique is less interesting for larger CO_2 contents.
Comparing the case of selling CH_4 with usage of CH_4 in combination with carbon capture (scenario 2b of chapter 3) at GLR = 1.5 Nm^3/m^3, the net revenues for selling CH_4 seem to be higher and the local emissions are lower than for the case with CH_4 usage.

5 Summary, conclusions and recommendations

5.1 Summary and Conclusions

In geothermal wells, greenhouse gasses are typically dissolved in the brine. If the geothermal well is operated with a separator and the greenhouse gasses are emitted into the atmosphere this reduces the sustainability of the geothermal energy. Therefore, in this report, three methods of handling the greenhouse gases were investigated: keeping the system under pressure, burning the methane for additional heat and electricity in a CHP in combination with carbon capture or capturing and injection the CO_2 in combination with selling the methane to the grid. In this work, both the technical aspects and the economic aspects of the greenhouse gas handling methods will be considered.

All three options are technically feasible. Keeping the system under pressure requires the least changes to the system and has the lowest land footprint – it does not require a relatively large carbon capture plant. At low gas-to-liquid (GLR) ratios, the required pressure at the topside to obtain an acceptable gas fraction of below 1% is modest at around 8 bar. Changing the topside system to be able to handle these pressures is relatively easy. The only major modification is in the increased power that is required by the ESP. Furthermore, this is the only option with the potential to avoid all emissions (if sustainable energy is used for the ESP). The carbon capture is never 100% efficient, such that always some greenhouse gasses are emitted.
The CHP in combination with carbon capture, on the other hand, requires a substantial carbon capture plant. If the captured CO_2 is then re-injected into the injection well, it also changes the pH in the fluid and eventually in the reservoir. The energy used by the carbon capture is also a significant fraction of the energy gained by burning the methane.
When selling the methane, the required capture plant for the CO_2-CH_4 separation is relatively modest, leading to a smaller land footprint and a more modest energy use compared to the energy content of the methane. Also, the pH in the injection well is not significantly altered, as the CO_2 content of the brine is not increased. Note that potential CO_2-emissions at the location where the sold CH_4 is used, is not taken into account.

When looking at the cost, of these options, burning the methane is typically the most expensive. The cost of a relatively small-scale carbon capture plant is large when considered per ton of CO_2 captured. Potentially carbon storage can be made feasible when combined with flue gas from other sources. The business case is not improved by including the 'bijstook' in the flue gas capture, as the capture plant will not be able to accommodate the larger differences in amounts of flue gas supplied between summer and winter, and because of this the capture plant has to be over-dimensioned in periods of low capture needs. Overall, the cost of the carbon capture and storage exceed the expected greenhouse gas emission costs for the foreseeable future.

At high gas fractions and large methane fractions, selling the methane to the grid can be profitable especially when the gas prices are relatively high. Since the gas from geothermal wells is typically mostly methane, carbon dioxide and nitrogen, carbon capture techniques can be used in order to separate the CO_2 from the methane. The high cost per ton of CO_2 are less of a problem, as the capture leads to revenue when selling the methane.

At low gas fractions or low methane content in the gas it is best to keep the system under pressure. The required topside pressure is not high when a small undissolved gas fraction of 1% is allowed at the topside. Therefore, the additional CAPEX of the changed topside design and the increased OPEX due to the electricity use of the ESP are limited compared to carbon capture or emission cost.

5.2 Recommendations

In this work, several options of handling the greenhouse gases from low-enthalpy geothermal wells were investigated, looking into both technical and economic aspects. A clear difference in the cost effectiveness of the different options was found, but there are still large uncertainties, especially in the costs. To obtain a more accurate analysis, the following points can be investigated further:

- Get a more accurate estimate of the costs to allow a higher pressure at the topside. This would require involving operators of geothermal wells and suppliers of topside equipment and ESPs.
- There are large uncertainties in the energy prices and the carbon prices, which affect the economics of all three options. A more economically focussed analysis could be performed in which the analysis is performed assuming different scenarios regarding the future energy supply and carbon pricing.
- In the calculations in this work, a very simple demand curve was assumed in which the heat demand in winter is twice that of the other seasons. This is a strong simplification: typically there are a relatively small number of days within the winter at which the heat demand is very high. This would make the carbon capture of the 'bijstook' even more difficult than what was assumed in the analysis in this report. It would therefore be good to look into combining the geothermal source with an HT-ATES system. This may allow a more constant heat production throughout the year, which can improve the business case of carbon capture (mainly scenario 2 from chapter 3).
- In the scenario where the methane is sold, more work should be done to determine how to handle trace components in the gas that might need to be separated from the methane in order for the methane to be sold.
- In this work, the option to utilize or sell the CO2 was not investigated. This might improve the business case for CCS.

Acknowledgements

We gratefully acknowledge the valuable input from the following persons:

- Dorien Dinkelman for talking through the whitepaper (Dijkstra et al., 2020; Dinkelman et al., 2021) on sustainable geothermal energy
- Cees Willems and Remco van Ee (Huisman) for their inputs in project meetings
- Jeffrey Haspels, Martin Hierl en Loek Schoenmakers (Vattenfall) for reviewing the report.
- Barry Irvine (Baker Hughes) for his input and discussions on the impact of higher pressure operations on electrical submersible pumps.

References

CBS. (2022). *No Title*. Aardgas En Elektriciteit, Gemiddelde Prijzen van Eindverbruikers. https://www.cbs.nl/nl-nl/cijfers/detail/81309NED?q=energiemarkt

Culberson, O. L., & McKetta, J. J. (1951). Phase Equilibria in Hydrocarbon-Water Systems III - The Solubility of Methane in Water at Pressures to 10,000 PSIA. *Journal of Petroleum Technology*, *3*(08), 223–226. https://doi.org/10.2118/951223-g

Dabiri, S., & Tryggvason, G. (2015). Heat transfer in turbulent bubbly flow in vertical channels. *Chemical Engineering Science*, *122*, 106–113. https://doi.org/10.1016/j.ces.2014.09.006

de Wildt, M. (2020). *Analysis of formation gas processing in geothermal projects (MSc thesis)*. Delft University of Technology.

Dijkstra, H., Dinkelman, D., Hanegraaf, M., Veldkamp, H., & Wees, J. D. van. (2020). *Whitepaper: Duurzaamheid van Geothermie in Warmtenetten*.

Dijkstra, H., Wasch, L. J., Regenspurg, S., Feldbusch, E., Iannotta, J., & Poort, J. (2021). *PERFORM deliverable D3.5 WP3: Report on CO2 injection and temperature optimization*.

Dinkelman, D., Dijkstra, H., de Simon, L., Ros, J., Hanegraaf, M., Veldkamp, H., & van Wees, J. D. (2021). *Factsheet Duurzaamheid Geothermie*.

Duan, Z., Møller, N., Greenberg, J., & Weare, J. H. (1992). The prediction of methane solubility in natural waters to high ionic strength from 0 to 250°C and from 0 to 1600 bar. *Geochimica et Cosmochimica Acta*, *56*(4), 1451–1460. https://doi.org/10.1016/0016-7037(92)90215-5

Gamboa, J., & Prado, M. (2012). Experimental study of two-phase performance of an electric-submersible-pump stage. *SPE Production and Operations*, *27*(4), 414–421. https://doi.org/10.2118/163048-PA

Ianotta, J., & Hehn, V. (2022). *DELIVERABLE 2.1 D2.1 Fluid data of geothermal sites (type C)*.

Jiang, Q., Heng, Y., Liu, X., Zhang, W., Bois, G., & Si, Q. (2019). A review of design considerations of centrifugal pump capability for handling inlet gas-liquid two-phase flows. *Energies*, *12*(6). https://doi.org/10.3390/en12061078

Kearns, D., Liu, H., & Consoli, C. (2021). *Technology readiness and costs of CCS*.

Konovalova, V. (2021). The effect of temperature on the corrosion rate of iron-carbon alloys. *Materials Today: Proceedings*, *38*, 1326–1329. https://doi.org/10.1016/j.matpr.2020.08.094

Lucile, F., Cézac, P., Contamine, F., Serin, J., Houssin, D., & Arpentinier, P. (2012). Solubility of Carbon Dioxide in Water and Aqueous Solution Containing Sodium Hydroxide at Temperatures from (293.15 to 393.15) K and Pressure up to 5 MPa: Experimental Measurements. *Journal of Chemical & Engineering Data*, *57*(3), 784–789.

Oh, S. Y., Binns, M., Cho, H., & Kim, J. K. (2016). Energy minimization of MEA-based CO2 capture process. *Applied Energy*, *169*, 353–362. https://doi.org/10.1016/j.apenergy.2016.02.046

Panterra. (2013a). *PVT ANALYSIS Draft Report Well HEK GTO1 S2 Zonneveld – rev 1 (obtained from nlog.nl)*.

Panterra. (2013b). *Well test analysis Well MDM-GT01 for ECW (available from nlog.nl)*.

Parkhurst, D. L., & Appelo, C. A. J. (2013). Description of input and examples for PHREEQC version 3—A computer program for speciation, batch-reaction, one-dimensional transport, and inverse geochemical calculations. In *U.S. Geological Survey Techniques and Methods, Book 6* (p. 497).

Prawoto, Y., Ibrahim, K., & Wan Nik, W. B. (2009). Effect of pH and chloride concentration on the corrosion of duplex stainless steel. *The Arabian Journal for Science and Engineering*, *34*(2C), 1–13. https://doi.org/10.1016/j.engfailanal.2007.11.003

Ros, J., & Monteiro, J. (2021). *CO2 Capture in Geothermal Application*.

Van ’t Spijker, H., & Ungemach, P. (2016). *Definition of Electrosubmersible pump (ESP) design and selection workflow* (Issue June).

Veldkamp, H., Goldberg, T., Bressers, P., & Wilschut, F. (2015). Identification of corrosion risk in the Netherlands. In *Operational issues in Geothermal Energy in Europe Annex II: Presentations* (p. 194).

Wasch, L. J., Dijkstra, H., Feldbusch, E., Regenspurg, S., Zotzmann, J., Iannotta, J., Poort, J., Twerda, A., & Shoeibi Omrani, P. (2022). Geothermal performance enhancement with pressure and temperature

control – field demonstration and predictive modelling. *Proceedings of the European Geothermal Congress 2022*.

Wasch, L. J., Shoeibi Omrani, P., Twerda, A., & Poort, J. (2021). *PERFORM deliverable D2.2 WP2: Report on the development and application of numerical model tools with the focus on CO2-(re)injection and pH control for scaling prevention and enhancing geothermal injectivity*.

Wikipedia.org. (2022). *Petra Nova*.

Zhang, W., Liu, H., Sun, Y., Cakstins, J., Sun, C., & Snape, C. E. (2016). Parametric study on the regeneration heat requirement of an amine-based solid adsorbent process for post-combustion carbon capture. *Applied Energy*, *168*, 394–405. https://doi.org/10.1016/j.apenergy.2016.01.049

Oh, S-Y , Binns, M., Cho, H., Kim, J.-K., Energy minimization of MEA-based CO_2 capture process, Applied Energy, 169, pg 353-362, 2016.

Appendix A: Including PHREEQC results in OLGA

OLGA can read fluid properties from a tab file. Such a file holds the properties of the gas, the oil and the water for a number of pressures and temperatures. Different programs can generate such tab files, in this work the program PVT Sim is used, which generates tab files containing the fluid properties for a matrix of 200 pressures and 200 temperatures. A single file is generated in PVT Sim for a brine containing NaCl at a concentration of 100 g/l, the highest NaCl concentration for which PVT Sim gave accurate results in Figure 4. In this PVT Sim simulation 1 Nm^3/m^3 of gas was added to the mixture, consisting of 80% methane and 20% carbon dioxide.

In the tab file generated by PVT Sim, the water properties are copied to the oil properties. In general there is no oil phase, making it possible to run the simulations in 2 phase mode in OLGA (only gas and 'oil'). This makes it easier to set the correct boundary conditions for the phase fractions. Next, PHREEQC calculations are performed in which the full brine composition and an accurate gas fraction is taken into account for each of the 200x200 pressures and temperatures in the tab file. From this calculation the liquid density and the gas fraction are taken and inserted into the tab file. These are the two most important parameters, since the density determines the hydrostatic pressure gradient in the well and the gas fraction determines whether problems can occur in the system due to the presence of gas. This procedure is summarized in Figure 27.

Note that when using this procedure, in OLGA the water fraction should be set to '0' everywhere. The hydrocarbon phase has exactly the properties of the brine and is in equilibrium with the vapor phase.

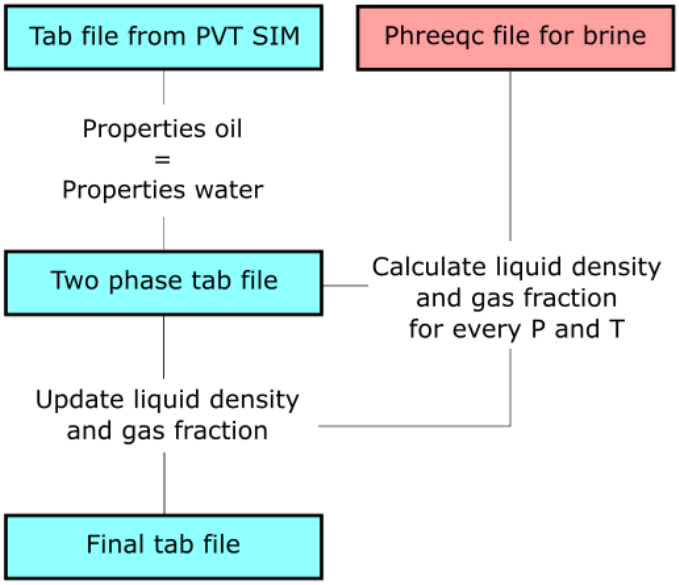

Figure 27: Summary of procedure to generate tab files.

The procedure to generate PHREEQC files based on fluid composition analyses from geothermal wells is presented in detail in appendix B.

Appendix B: Setup and tuning of the PHREEQC model

Geochemical simulations of the geothermal fluid requires input data for the brine composition and the (outgassed) gas composition. For a bottom hole sample, the gas is released from the brine at around room temperature. At room temperature and 1 bar pressure, a part of the gas will remain in solution. The remaining dissolved methane is usually not measured and this has to be corrected for in the model. The dissolved carbon dioxide is measured as HCO_3^-, but the measurements are often inaccurate and may be further affected by calcite precipitation after sampling. For example, measured HCO_3^- concentrations may vary between 100 and 600 mg/l for a single well. Because of the uncertainty in measurements of dissolved CO_2 and the absence of measurements of dissolved methane and nitrogen, it is more accurate to calculate these concentrations with PHREEQC (Dijkstra et al., 2021; Wasch et al., 2021, 2022).

The concentrations of dissolved gas phases can be calculated by equilibration with the gaseous phases according to their partial pressures. This calculation is very sensitive to the salinity, temperature and – in case of CO_2 – to the initial pH of the solution. The pH is again a value with large uncertainties and may vary between 5 and 6 for different measurements of brine from the same well. The pH could be measured on site to increase the accuracy, but this is often not done. The most accurate pH measurements of (CO_2 containing) brines are of in situ measurements with a bypass measurement device. When only an inaccurate pH value is available, this value can be calibrated within PHREEQC to the more accurate CO_2 fraction measurement. The initial pH is also a strong control on calcite precipitation and hence if a pressure threshold (below which CO_2 outgassing increases the pH to the extent that calcite precipitates) is known for the geothermal site, this data can be used for model calibration (Dijkstra et al., 2021; Wasch et al., 2021, 2022)(Panterra, 2013b)

To calibrate the model, the gas fractions are taken as the most reliable data and the model is adapted to reproduce these numbers. The model is setup by defining a solution with the measured brine composition, pH, density, temperature and dissolved gas in equilibrium with the CO_2, CH_4 and N_2 partial pressures. Secondly, a gas is defined with a fixed pressure of 1 bar and CO_2, CH_4 and N_2 partial pressures as well as a volume according to the measured gas water ratio (GWR). The gas phase and solution are equilibrated together at reservoir pressure and temperature and when combined reflect the fluid in the reservoir. If the model is correctly set-up, simulating bringing this reservoir fluid to lab conditions will yield the gas composition and GWR as measured. If there is a deviation, the model can be calibrated by adjusting the controlling input parameters (with inherent uncertainties) as discussed above.

There are some general trends for adjusting parameters to match the CO_2 content and total gas volume:

- Decreasing the initial solution temperature, increases the gas volume and CO_2 fraction.
- Increasing the initial solution pH, increases the gas volume and CO_2 fraction.
- Increasing the Gas Phase temperature, increases the gas volume.

Note that the last parameter is actually a condition during measurement. Gas fractions are reported for normal conditions (0˚C and 1 bar), and hence a temperature of 0˚C is used for the Gas Phase.

Middenmeer

The MDM-GT-01 bottom hole sample was used for the fluid () and gas () composition. Note that only the elements included in the Pitzer database could be used in the simulation.

Table 23. Water composition of the Middenmeer geothermal fluid.

Element	Concentration (mg/l)
Na	47780
K	718
Ca	8588
Mg	1260
Ba	4.12
Sr	453
Fe	70.28

The model was calibrated in several steps. The initial solution temperature was increased from room temperature to 25 ˚C (equal to the temperature of pH measurement). The pH was decreased from the measured value of 6 to 5.7 to match the subsequently calculated CO_2 fraction in the gas at lab conditions. To make sure the model does not predict calcite scaling at high pressures (as this is not observed by the operator), the initial solution pH was further decreased from 5.7 to 5.5. With a pH of 5.5, the simulated calcite scaling pressure threshold is 3 bar, with scaling occurring at lower pressures. No observations or experiments are available for the calcite scaling pressure threshold to more precisely calibrate the initial solution pH. Table 24 below shows the accuracy of the calibrated PHREEQC model for simulating of the gas fractions and gas volume.

Table 24. Measured and modelled gas composition of the Middenmeer geothermal fluid.

	Measured		Measured	Simulated
	mol%		Normalized to 1 bar	
CO_2(g)	0.098		0.108	0.102
Mtg(g)	0.751		0.823	0.828
Ntg(g)	0.064		0.070	0.070
Volume (GWR)	0.41			0.39

The model is used to calculate outgassing with different pressures. The simulated bubble point is at 19 bar (Figure 28 a). This is in agreement with the bubble point as calculated by Panterra (2013):

“To calculate the solubility of methane, two different models are used, viz., Henry’s Law and an equation of state. Moreover, the solubility of methane in water at the standard conditions is used to show that the bubble-point pressure must be much higher than the atmospheric pressure. The two models give similar values of 21 bar (+/- 20%) for the bubble-point pressure corresponding to a gas/water ratio of 0.4 m^3/m^3 at T = 90 °C.”

Measurements of gas fractions with different pressures are required to assess the accuracy of the predictions of outgassing with different pressures. The model indicates a GWR of 0.08 for 5 bar and a GWR of 0.25 for 2 bar (Figure 28 a). Data is available for GWR and gas composition of surface samples taken at 2 bar and 5 bar, however the data is inconsistent. The GWR ratio is smallest at 2 bar (0.098), although the lowest pressure should release the most gas. Furthermore, the GWR is increasing from 0.1 to 0.13 to 0.14 for the three different samples taken at 5 bar. This suggests issues with the sampling, for example that equilibrium was not achieved in the separator tank during sampling.

The measured CO_2 fractions vary from 43% at 2 bar to 30% at 5 bar and are considerably higher than the simulated CO_2 fractions of 13% at 2 bar and 9% at 5 bar (Figure 28 b). These differences could again indicate issues with sampling and/or analyses. Although the measured and modelled fractions are far apart, both do show a higher CO_2 fraction with decreasing pressure. This is as expected since the less soluble methane and nitrogen have a larger tendency to partition into the gas phase at the onset of pressure release.

The outgassing of CO_2 leads to an increase of the pH which increases the calcite scaling tendency (Figure 28 c,d). As discussed before the model was calibrated to achieve a calcite scaling pressure threshold of 3 bar, below which the saturation index becomes positives meaning that calcite tends to precipitate.

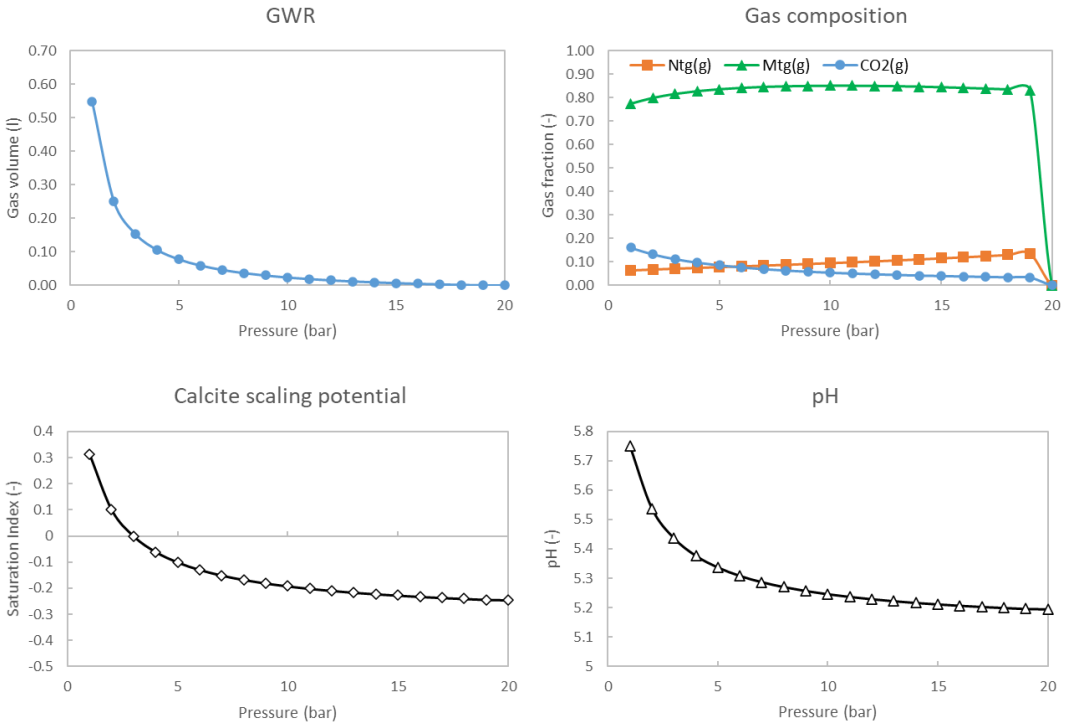

Figure 28 PHREEQC simulation results with a changing topside pressure. Results are shown of: a) the gas water ratio (GWR), b) the gas composition, c) the calcite scaling potential and d) the pH.

Heemskerk

For the Heemskerk model, data from three different samples and analyses were combined. The density, GWR and gas composition was taken from the bottomhole sample (Panterra, 2013a). The pH and fluid composition (Ianotta & Hehn, 2022) were taken from two different analyses.

Table 25: Water composition of the Heemskerk geothermal fluid.

Element	Concentration (mg/l)
Na	93000
K	1300
Ca	9500
Mg	740
Ba	9.0
Sr	310
Fe	131
Cl	170000
S(6)	390
Mn	12.8

Li	26.9
Si	9.37

Even when selecting these data from different available sources, the model does not require further calibration with respect to the gas content. However with these input parameters, calcite scaling is predicted occur over the entire production well (at P>331 bar). To make sure the model does not predict calcite scaling at high pressures (as this is not observed by the operator), the initial solution pH was decreased from 5.275 to 5.1. With a pH of 5.1, the simulated calcite scaling pressure threshold is 5 bar, with scaling occurring at lower pressures. No observations or experiments are available for the calcite scaling pressure threshold to more precisely calibrate the initial solution pH.

Table 26 shows the accuracy of the simulation of the gas fractions and gas volume with the PHREEQC model.

Table 26: Measured and modelled gas composition of the Middenmeer geothermal fluid.

	Measured	Measured	Simulated
	mol%	Normalized to 1 bar	
CO_2(g)	0.2566	0.2747	0.2751
Mtg(g)	0.5721	0.6124	0.6120
Ntg(g)	0.1056	0.1130	0.1129
Volume (GWR)	0.36		0.36

The model is used to calculate outgassing with different pressures. The calculated bubble point is at 16 bar (Figure 29a). With further pressure decrease the relative amount of CO_2 (mol%) increases (Figure 29b). This is as expected since the less soluble methane and nitrogen have a larger tendency to partition into the gas phase at the onset of pressure release. Model calibration for the gas fractions is not possible since there are no gas analyses available of gas released at different pressures.

The outgassing of CO_2 leads to an increase of the pH which increases the calcite scaling tendency (c,d). As discussed before the model was calibrated to achieve a calcite scaling pressure threshold of 5 bar, below which the saturation index becomes positives meaning that calcite tends to precipitate.

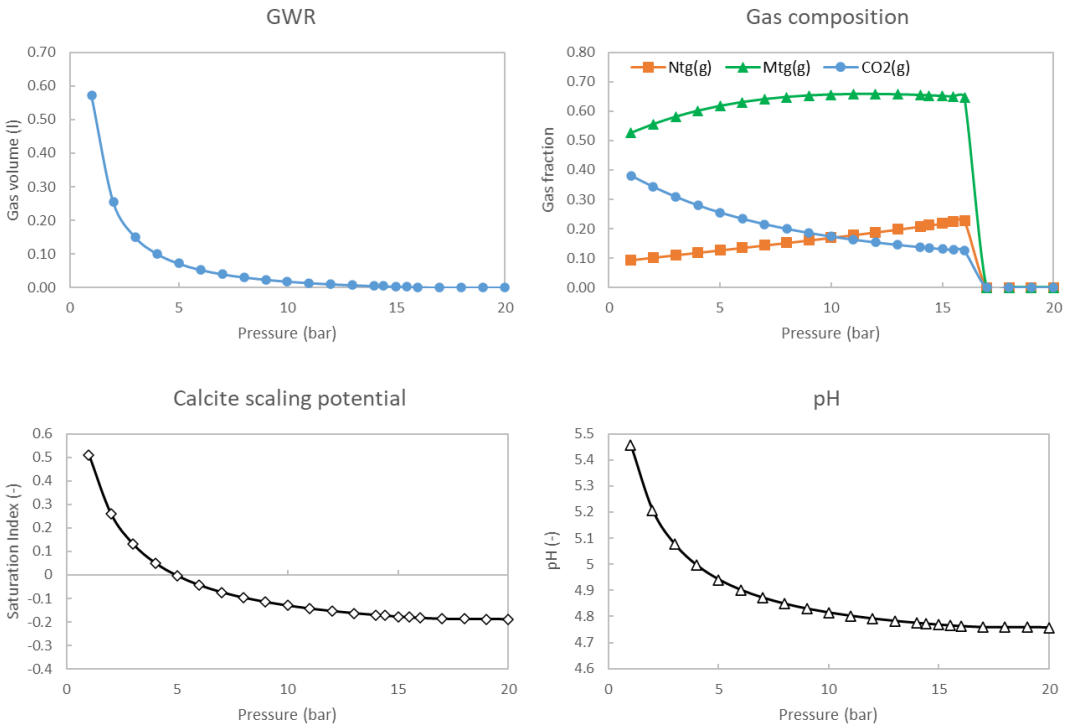

Figure 29: PHREEQC simulation results with a changing topside pressure. Results are shown of: a) the gas water ratio (GWR), b) the gas composition, c) the calcite scaling potential and d) the pH.

Discussion

For all geochemical models the Pitzer thermodynamic database was used. This database is generally regarded as accurate for higher salinities, but lacks solubility data for many metal compounds and aluminosilicates. Different thermodynamic databases are built for specific conditions or applications and can yield widely different results for the same geochemical model. Considering the good fit of the models for gas solubility using the Pitzer database, other databases were not considered. However, precipitation of for example aluminosilicates, chlorides and metal sulphides cannot be simulated with this database but are common scale minerals.

Deviations between measured and simulated compositions can have a multitude of reasons. One is the use of equilibrium in the model, neglecting the effect of reactions rates (kinetics). Gas separation may be kinetically controlled but data and rate equations are scarce. Also note that kinetics may cause errors in gas measurements as equilibrium may not have been achieved during sampling or before analysis.

Appendix C: CO_2 separation

CO_2 separation is required when CO_2 is to be injected into the reservoir (chapter 3), but also when the methane in the geothermal gas is sold to the grid. There are several techniques available that enable CO_2 separation, but the most robust method is scrubbing [(11)]. Scrubbing typically results in a separation efficiency of about 90%.

With scrubbing, the gas is fed into an adsorber column, where the CO_2 is dissolved into a solvent. The CO_2-rich solvent then passes to the stripper where the CO_2 is released from the solvent. To release the CO_2 the solvent in the stripper needs to be heated up, which is a major part of the total energy consumption of the process (~50%). Several solvents are available, but Mono-Ethanol-Amine (MEA) is considered to be the industry benchmark due to its low cost, high reaction rate with CO_2, and the large experience with it (Oh et al., 2016).

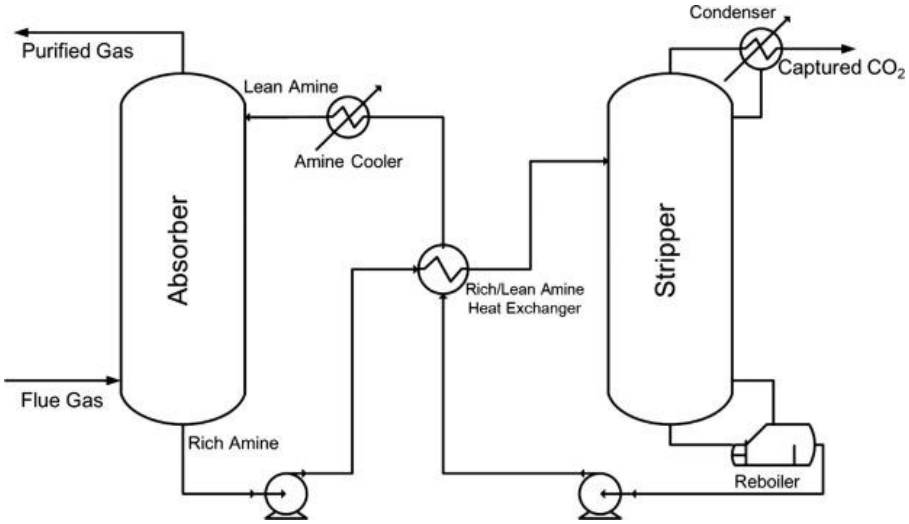

Figure 30: Schematic overview of the elements required for scrubbing of CO_2.

In the work by Ros & Monteiro (2021) a complete combustion of the geothermal gases is done in a Combined Heat and Power (CHP) plant resulting in a flue gas outflow with 4.2 mol% CO_2 (typical value for CHP). Then the CO_2 is separated from the flue gas. They build a model of the separation process in ProTreat to assess the technical and financial aspects, which are also based on 'experience numbers'. Here the CAPEX of a CO_2-separation plant (amine-based) including compressors for the reinjection of CO_2 in the geothermal injection stream is estimated as (based on Kearns et al. (2021)):

$$CAPEX = 13\, W^{0.7}$$

where W is the captured CO_2 mass flow rate in ton/h. The power of 0.7 results in an increase in CAPEX of 60% for a doubling of the captured flow rate (note: Kearns et al. (2021)mentions an increase of 50% for doubling of the captured flow rate). The prefactor of 13 is set to obtain a CAPEX of 13 M€ for a capture flow rate of 1 ton CO_2/h, and a CAPEX of 40 M€ for a capture flow rate of 5 ton CO_2/h.

[11] Membrane technology to separate CO_2 functions best if the partial pressure of CO_2 is relative large (e.g. ~1 bar or more), and operates best with higher CO_2 fractions than considered in this report (< 10 mol%).

Note that when using this estimate for the CAPEX for the large scale CCS project Petra Nova (capturing 1.6 Mton CO_2/y, CAPEX of ~1 G€,Wikipedia.org (2022)), the estimated CAPEX is 0.5 G€ (using 8760 operational hours per year). For the CCS project Boundary Dam (capturing 1 Mton CO_2/y, CAPEX of ~1.5 G€,Wikipedia.org (2022)), the estimated CAPEX is ~0.36 G€ (using 8760 operational hours per year). Thus the estimated CAPEX seems to give a low estimate.

The CAPEX, the annual interest rate, p, and the life time of the plant in years, T, are used to compute the equivalent annual CAPEX via:

$$equivalent\ annual\ CAPEX = CAPEX\ \frac{p}{1-(1+p)^{-T}}$$

Where an interest of 8% and a plant lifetime of 30 years has been assumed by Ros & Monteiro (2021).

For CO_2 capture from the flue gas exiting the CHP the total heat required for the plant is about 3.9 GJth/ton CO_2 (Zhang et al., 2016). The total electricity required for the capture plant is about 300 kWh_e/ton CO_2 (~130 kWh_e/ton CO_2 for the compression of the flue gas from 1 bara at the CHP outflow to 1.5 bar at the capture plant inlet [12], ~90 kWh_e/ton CO_2 for the amine recirculation (ref 3), and ~80 kWh_e/ton CO_2 for the compression of CO_2 from 1 bara at the capture plant outlet to 40 bara at the point of reinjection [13]). An electricity cost of 0.1 €/kWh (= 27.8 €/GJ) and a heat cost of 0.014 €/kWh (= 4 €/GJ) are used to estimate the variable OPEX. This amounts to about 45.6 €/ton CO_2. The fixed OPEX is estimated as 30% of the equivalent annual CAPEX.

For separation of CO_2 from the methane in the geothermal gas the required electrical energy is expected to be lower as the gas streams are much lower. The power required to 'push' the geothermal gas to the capturing unit is reduced from ~130 kWh_e/ton CO_2 to ~65 kWh_e/ton CO_2 [14]. This reduces the variable OPEX to about 235 kWh_e/ton CO_2. With the amount of heat required unchanged compared to the CO_2 capture from the flue stream after combustion the total variable OPEX amounts to ~39 €/ton CO_2.

[12] Assuming 4.2 mol% CO_2 and 95.8mol% N_2, a polytropic process in the compressor of 1.2 and compressor efficiency of 70%.
[13] Assuming pure CO_2, a polytropic process in the compressor of 1.2 and a 3 stage compressor with intercooler and efficiency of 70%.
[14] Assuming 9 mol% CO_2 and 95.8mol% N_2, a polytropic process in the compressor of 1.2 and compressor efficiency of 70%.

Appendix D: CO_2 balance

CO_2 is highly soluble in water. Once dissolved it reacts with water to H_2CO_3, which itself also reacts with water to HCO_3^- and CO_3^{2-}. The pH can be solved using the hydration constant, K_h, the acid dissociation constants, K_{a1} and K_{a2}, and assuming the dissolved H+ originates only from carbonic acid dissociation (Wikipedia.org).

$K_h = [H_2CO_3] / [CO_{2,aq}] = 1.7\ 10^{-3}$

$K_{a1} = [HCO_3^-][H^+] / [H_2CO_3] = 2.5\ 10^{-4}$ mol/L

$K_{a2} = [CO_3^{2-}][H^+] / [HCO_3^-] = 4.69\ 10^{-11}$ mol/L

This can be rewritten to (Bjerrum plot equations for the carbonate system (Wikipedia.org)):

$$[CO_{2,aq}] / DIC = [H^+]^2 / ([H^+]^2 + K_h K_{a1} [H^+] + K_h K_{a1} K_{a2})$$

$$[HCO_3^-] / DIC = K_h K_{a1} [H^+] / ([H^+]^2 + K_h K_{a1} [H^+] + K_h K_{a1} K_{a2})$$

$$[CO_3^{2-}] / DIC = K_h K_{a1} K_{a2} / ([H^+]^2 + K_h K_{a1} [H^+] + K_h K_{a1} K_{a2})$$

With $DIC = [CO_{2,aq}] + [HCO_3^-] + [CO_3^{2-}]$ the total dissolved inorganic carbon in the system.

Assuming that all H^+ comes from the dissociation of H_2CO_3, the concentration of H^+ is equal to :

$[H^+] = [HCO_3^-] + 2\ [CO_3^{2-}]$

For a 54 Nm^3/h CO_2 gas flow originating from a total of 400 m3/h brine, the original solution has a DIC = 0.0055 mole/L. Using the above equations this results in [H+] = $6.85\ 10^{-5}$ mol/L or pH = 4.2 (i.e. $pH = -\log_{10}([H^+])$. Likewise a 595 Nm^3/h CO_2 gas flow in a 400 m^3/h brine will result in pH = 3.8 and a 1980 Nm^3/h CO_2 gas flow in a 400 m^3/h brine will result in pH = 3.5.

WARMINGUP
Innovatief Duurzaam Warmtecollectief

Adres
Princetonlaan 6
3584 CB Utrecht

Postadres
Postbus 80015
3508 TA Utrecht

Telefoon
088 866 42 56

E-mail
contact@warmingup.info

Website
www.warmingup.info

WARMINGUP

Innovatief Duurzaam Warmtecollectief

Addendum to ‘Handling greenhouse gases from geothermal wells’

door
Darren Jones and Dries van Nimwegen
21 december 2023

Addendum to ‘Handling greenhouse gases from geothermal wells’

Darren Jones and Dries van Nimwegen
21 december 2023

Dit project is uitgevoerd als onderdeel van het Innovatieplan WarmingUP. Dit is mede mogelijk gemaakt door subsidie van de Rijksdienst voor Ondernemend Nederland (RVO) in het kader van de subsidieregeling Meerjarige Missiegedreven Innovatie Programma’s (MMIP), bij RVO bekend onder projectnummer TEUE819001.
WarmingUP geeft invulling aan MMIP-4 – Duurzame warmte en koude in gebouwde omgeving en levert daarmee een bijdrage aan Missie B – Een CO_2-vrije gebouwde omgeving in 2050.

Projectnummer
060.43190/01.01.02

Keywords
Geothermal energy, sustainability, geothermal wells

Jaar van publicatie
2023

Meer informatie
Lies Peters
E Lies.peters@tno.nl

Introduction

This is an addendum to the report on handling greenhouse gases (both CO_2 and methane) from geothermal wells as part of the WarmingUP project (Nimwegen et al., 2022). This report considered three methods of avoiding greenhouse gas emissions from geothermal wells:

- Keeping the system under pressure, such that the gasses do not escape from the geothermal brine and are reinjected
- Burning the methane, capturing the CO_2 and either reinjecting the CO_2 into the injection well or storing the CO2 at another location
- Selling the methane and reinjecting the CO2. Note that to avoid greenhouse gas emissions the buyer of the methane should perform carbon capture.

It was concluded by Nimwegen et al. (2022) that keeping the system under pressure is likely the most cost effective option, especially at low gas fractions. However, the cost estimates for this option were poorly substantiated. The goal of this addendum is to include additional information on the cost aspects of keeping the system under pressure for an improved cost estimate. To determine these costs it is first required to determine which pressure is required. In the report it was assumed that a void fraction of 1% is acceptable in topside equipment. It would not significantly change the performance of pumps, heat exchangers and filters. Such a void fraction occurs at pressures of around 8 bar for low gas fractions (0.33 Nm^3/m^3) and around 25 bar for high gas fractions (1 Nm^3/m^3).

Keeping the system under pressure changes the CAPEX and OPEX of the geothermal well. The OPEX is related to the change in electricity consumption of the ESP and the injection pump, which can be estimated relatively well, and changes in maintenance costs. The CAPEX was estimated in the thesis of de Wildt (2020), who estimated 30,000 EUR per bar of increased pressure. In this addendum the CAPEX and OPEX costs related to keeping the system under pressure are investigated further.
In the third chapter, the greenhouse gasses are separated from the brine and then further split into CO_2, CH_4 and other components. The CH_4 is then sold to the market. It is determined whether this could be profitable. Note that the sale of the CO_2 is not considered and the emission of the party buying the methane is considered out of scope of the current analysis.

Since the assessment of the various options differs, they cannot be compared directly. Instead an attempt is made to assess the impact of a certain option with respect to a relevant base case, which can differ per option.

Overview of topside equipment

A summary of the typical top side equipment for a geothermal doublet system is shown in Figure 1. In order to gain a good understanding of the top side equipment, their costs and associated pressure ratings, interviews were conducted with geothermal specialists across The Netherlands. In addition, the available literature was reviewed. The outcomes are summarised in Table 1 which show the OPEX, CAPEX and pressure ratings for the typical top side equipment components. It is important to note that exact costs will vary depending on the system e.g. fluid properties, target depth of the system, design, location, heat demand and energy price.

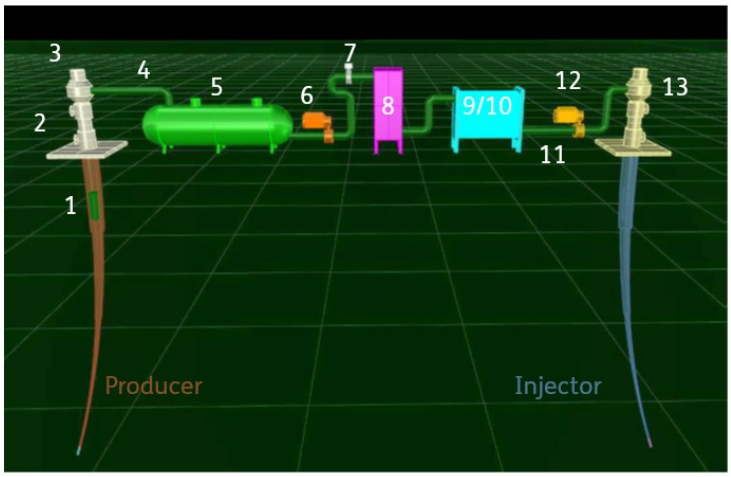

1 – ESP
2 – Production well head
3 – Injector point
4 – Piping (hot water)
5 – Degasser
6 – Booster pump
7 – Monitoring system
8 – Filter
9/10 – Heat exchanger/heating network connection
11 – Piping (cold water)
12 – Injector pump
13 – Injection well head

Figure 1: Schematic overview of the top side equipment for a typical doublet geothermal system (adapted from Com2Geo report – TNO 2023 R10385)

Table 1: Summary of typical top side equipment and associated costs and pressure ratings.

Type	CAPEX (€)	OPEX (€ per year)	Pressure ratings (bar)
ESP	300,000-500,000	65,000-95,000	10-30
Well head	85,000	3,000	100 (200 – drilling)
Pipeline	300,000	Unknown	10 (minimum)
Degasser/Separator	300,000-500,000	20,000	10 (minimum)
Filter	260,000	30,000	10 (minimum)
Heat exchanger	360,000	Unknown	16-24 (maximum)
Injector pump	150,000-250,000	Unknown	25-90

Cost analysis

The changes in CAPEX when keeping the system under pressure are:

- The degasser/separator is no longer required
- For pressures above 10 bar equipment with a higher pressure rating is required
- The ESP needs to increase the pressure more
- If the topside pressure is sufficiently high it may be possible that the injector pump is no longer required

The change in CAPEX is summarized in Table 2 for both the low and the high gas fractions. For low gas fractions there is a large cost saving because the separator is no longer required. Since the system is not operated at a pressure above the rating of the current components, no additional costs need to be made. For the high gas fraction more changes are required. The ESP needs to be more powerful to obtain a higher pressure. To estimate the additional costs, the range of costs for the ESP is taken from Table 1 (instead of a cheap now an expensive ESP is selected). Note that this is a very rough estimate. For the cost of the higher pressure rating above 10 bar, the estimate by de Wildt (2020) is used. In the report by de Wildt (2020) it was determined that at operation at 25 bar an injection pump is no longer required, leading to a significant cost saving. Depending on reservoir pressure and injectivity, however, this may not

be the case. This analysis therefore holds for the example in the report but is not truly general. At the bottom line, keeping the system under high pressure leads to a modest cost increase.

Table 2: Rough estimates of CAPEX differences for systems that are designed to operate under pressure. Green indicates cost savings, while red indicates additional costs.

Item	Low gas fraction (< 10 bar)	High gas fraction (25 bar)
Degasser/Separator	€ -400,000	€ -400,000
Equipment pressure rating	€ 0	€ 30,000 per bar above 10 bar -> €450,000
ESP	€ 0	€ 200,000
Injector pump	€ 0	€ -200,000 0
Total	€ -400,000	€ 50,000

The differences in OPEX related to keeping the system under pressure are presented in Table 3. Calculations are based on an electricity price of €0.1/kWh and on 6,000 operational hours per year. The differences in power consumption were calculated in the report and are summarized in Table 5 and Table 6 in the report (Nimwegen et al., 2022).

For the OPEX of the equipment pressure rating 10% of the purchasing cost is used. These are not the active components (such as pumps), such that not too much replacement and repair should be required. To determine the difference in OPEX for the ESP, the range from Table 1 is taken as the difference between an expensive and a cheap ESP. Again, this is a very rough estimate. For the ESP the OPEX costs are 20% of the CAPEX cost. This same ratio was taken for the injector pump.

Table 3: Rough estimates of annual OPEX differences for systems that are designed to operate under pressure. Green indicates cost savings, while red indicates additional costs.

Item	Low gas fraction (< 10 bar)	High gas fraction (25 bar)
Degasser/Separator	€ -20,000	€ -20,000
Equipment pressure rating	€ 0	€ 45,000
ESP	€ 0	€ 30,000
Injector pump	€ 0	€ -40,000 0
Electricity costs	€ 90,000	€ 114,000
Total	€ 70,000	€ 129,000

To come to a total annual cost overview, an annual equivalent CAPEX is calculated based on a 30 year depreciation with 8% interest. This leads to the numbers in Table 4. This shows that the annual cost of keeping the system under pressure is relatively independent of the pressure, because the injection pump is no longer required in the considered high pressure system. Note that when the injection pump cannot be removed, this leads € 58,000 of additional annual costs.

Table 4: Total additional annual costs for keeping the system under pressure.

Item	Low gas fraction (< 10 bar)	High gas fraction (25 bar)
OPEX	€ 70,000	€ 129,000
Annual equivalent CAPEX	€ -35,500	€ 4,500
Total	€ 105,500	€ 133,500

These estimates are a little bit lower than those made in the report. However, they are still relatively uncertain. To obtain better estimates system designs need to be made, such that quotations can be requested for the actual components. The conclusion that operating under pressure is cheaper than using a CHP and carbon capture remains valid in this updated analysis. At high gas prices, however, it can still be beneficial to sell the methane instead of keeping it under pressure.

Additional remarks

In the interviews several additional issues were raised, which are not taken into account in the current analysis. The cost estimates can be improved if the costs related to these points can be quantified.

- Keeping the system under pressure has other advantages such as having larger concentrations of CO_2 in solution which may help to mitigate scaling.
- The separator can be left out when keeping the system under pressure, but additional by-passes and valves may be required.
- The weakest topside component is likely to be the heat exchanger which can cope with typically up to a maximum of 16 bars.
- Additional ESP downtime may be expected as the load on the ESP is increased.

There is already experience with operating systems in the Netherlands under pressure. The geothermal doublet at Heemskerk (wells HEK-GT-01 and 02) is not degassed and operated at a pressure of around 8 bar (Webinar: Duurzaamheid geothermie in warmtenetten | TNO).

Acknowledgements

We gratefully acknowledge the valuable input from the following experts: Geert Jan van Og, Pejman Shoeibi Omrani and Floris Degener.

References

Nimwegen, D. van, J. van 't Westende, P. Shoeibi Omrani, L. Wasch and E. Peters (2022) Handling greenhouse gases from geothermal wells. WarmingUP report. WarmingUP T4A handling greenhouse gases (accessed 21/12/2023)

TNO (2023). Feasibility of complete composite geothermal well systems. Com2Geo. R19385.

Wildt, M. de (2020). *Analysis of formation gas processing in geothermal projects (MSc Thesis).* Delft University of Technology.

WARMINGUP
Innovatief Duurzaam Warmtecollectief

Adres
Princetonlaan 6
3584 CB Utrecht

Postadres
Postbus 80015
3508 TA Utrecht

Telefoon
088 866 42 56

E-mail
contact@warmingup.info

Website
www.warmingup.info